NATIONAL ACADEMY OF SCIENCES OF UKRAINE
Palladin Institute of Biochemistry

BIOTECHNOLOGIA ACTA

Vol. 16, No 2, 2023

BIMONTHLY

Editorial address:
Palladin Institute of Biochemistry of the NAS of Ukraine, 9, Leontovich Street, Kyiv, 01054, Ukraine;
Tel.: +3 8 044–235–14–72; ***E-mail:*** biotech@biochem.kiev.ua; ***Web-site***: www.biotechnology.kiev.ua

According to the resolution of the Presidium of the National Academy of Sciences of Ukraine from 27.05.2009 №1-05 / 2 as amended on 25.04.2013 number 463 Biotechnologia Acta has been included in High Attestation Certification Commission list of Ukraine for publishing dissertations on specialties "Biology" and "Technology".

Certificate of registration of print media КВ series №19650-9450ПР on 01.30.2013

Literary editor — H. **Shevchenko**; Computer-aided makeup — **O. Melezhyk**
Authorized for printing 2023/04/28, Format — 210×297. Paper 115 g/m^2. Gaqrn. SchoolBookC. Print — digital. Sheets 11.6. An edition of 100 copies. Order 2.6. Make-up page is done in Palladin Institute of Biochemistry of the National Academy of Sciences of Ukraine. Print — **O. Moskalenko** FOP

NATIONAL ACADEMY OF SCIENCES OF UKRAINE
Palladin Institute of Biochemistry

BIOTECHNOLOGIA ACTA

Scientific journal

Bimonthly

Vol. 16, No 2, 2023

Conference abstracts
"CURRENT PROBLEMS OF BIOCHEMISTRY AND BIOTECHNOLOGY — 2023"
dedicated to the 120th anniversary of the birth of the outstanding Ukrainian biochemist D. L. Ferdman

НАЦІОНАЛЬНА АКАДЕМІЯ НАУК УКРАЇНИ
Інститут біохімії ім. О. В. Палладіна

BIOTECHNOLOGIA ACTA

Науковий журнал

Том 16, № 2, 2023

Тези конференції
«АКТУАЛЬНІ ПРОБЛЕМИ БІОХІМІЇ
ТА БІОТЕХНОЛОГІЇ — 2023»,
присвячена 120-річчю з дня народження видатного
українського біохіміка Д. Л. Фердмана»

UDC 577.29 https://doi.org/10.15407/biotech16.02.007

SYNTHESIS OF CALIX[4]ARENES WITH FIXED CONFORMATION AS POTENTIAL INHIBITORS OF FIBRIN POLYMERIZATION

D. M. AHISHEV[1, 2, 3], *O. O. HRABOVSKYI*[1]

[1]Palladin Institute of Biochemistry
of the National Academy of Sciences of Ukraine, Kyiv
[2]Institute of Organic Chemistry
of the National Academy of Sciences of Ukraine, Kyiv
[3]Kyiv National Taras Shevchenko University, Ukraine

E-mail: agdmytro@gmail.com

Received 2023/03/23
Revised 2023/04/12
Accepted 2023/04/28

Intravascular thrombus formation is one of the main causes of such deadly diseases and pathologies as ischemic heart disease, ischemic stroke, pulmonary embolism, atrial fibrillation, and venous thromboembolism [1, 2].

That is why the development of new approaches for preventing intravascular blood coagulation is an important task for biochemistry and biotechnology. Most of biomolecules that target clotting factors. However, in our study we focused on another type of molecules, which are direct inhibitors of fibrin polymerization.

As a scaffold, we have used a calix[4]arene molecule because of its tunable diversity at both upper and lower rims, its pre-organized nonpolar cavities, pre-organized ion-bonding sites and well-defined conformations [3]. Previously we have shown that calix[4]arenes are active inhibitors of fibrin polymerization process. Binding to the 'A'-knob of fibrin desAB molecule calix[4] arenes prevents knob-hole interactions between different fibrin molecules thus suppressing clotting. Recent studies proved the efficacy of sodium salt of 5, 11, 17, 23-bis(dihydroxyphos phoryl)methylcalix[4]arene (C-145) as an effective anticoagulant agent [4, 5].

Molecular dynamic studies of C-145 demonstrated the importance of conformation of the macrocycle for its fibrin-binding activity. In particular calyx[4]arene has two different conformations of its cup (the macrocycle) that can be described as '*1,3-alternate*' (opened) or '*conus-conformation*' (fixed).

Aim. The purpose of the present study was to develop a method for the fixation of 'fixed' conformation for estimation of the impact of calix[4]arene structure on the efficacy of its anticoagulant activity. This was achieved by substitution of the lower rim of C-145 analogue.

Metods. Calix[4]arene C-145 was obtained according to the method described in [6] with one additional step that included Mitsunobu reaction in order to obtain disubstituted calixarene C-145F (Fig. 1).

Modeling of 3D-structure of calix[4]arene C-145 and its analogue C-145F was performed in Maestro, Schrodinger software.

Calix[4]arene C-145F (compound 6) was obtained in 4 steps starting with Duff reaction. Calix[4]arene methylene-bis-phosphonic ester 3 was prepared via addition of diisopropylphosphite in presence of metallic sodium to the parent calix[4]arene aldehyde 2. Further steps included Mitsunobu reaction, that afforded dipropoxycalix[4]arene 5 with rather good yields (80%), following the hydrolysis step that resulted in compound 6 in almost quantitative yield.

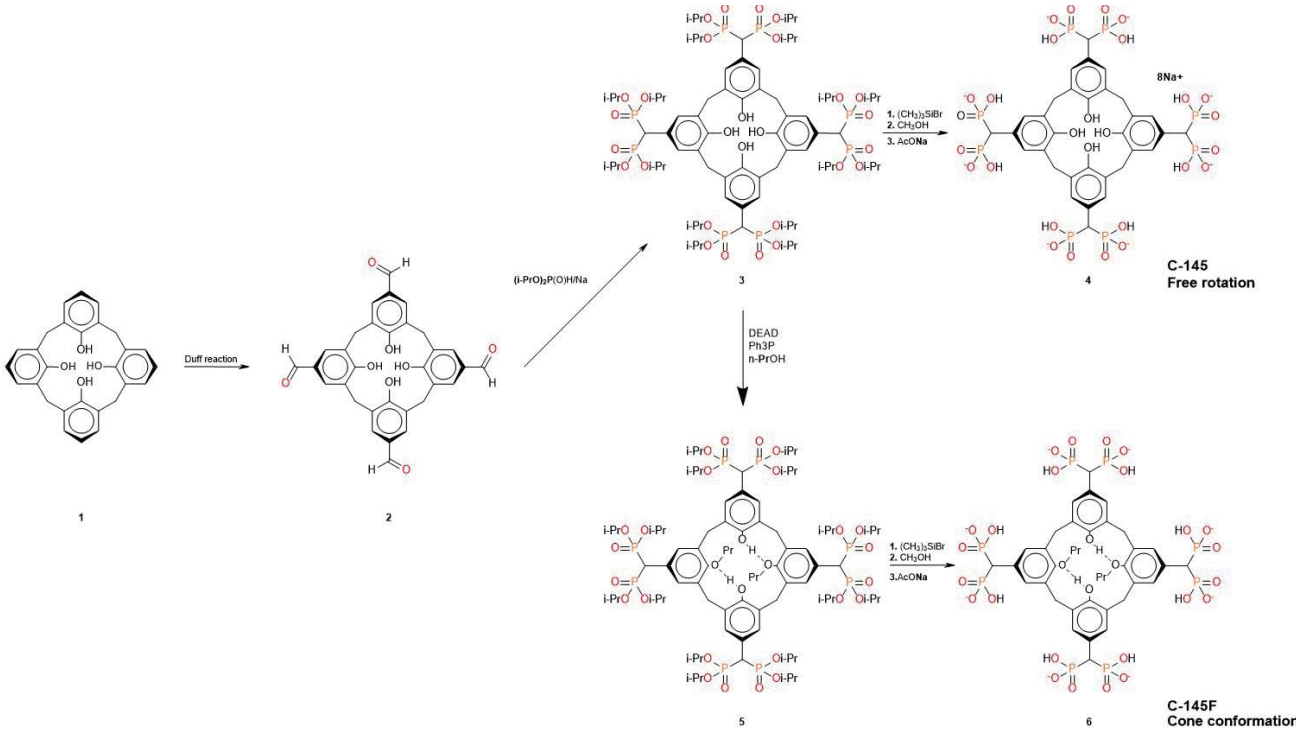

Fig. 1. **Synthesis of calix[4]arenes C145 and its analogue C145F with lower rim substitution**

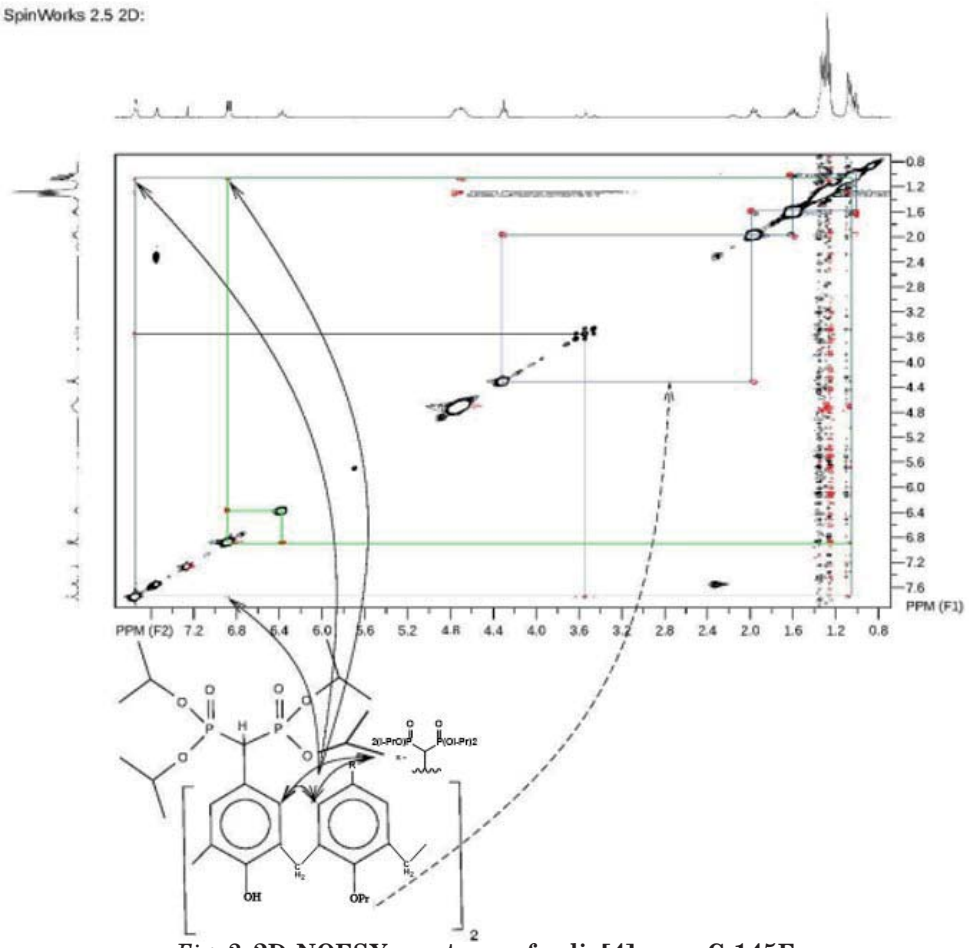

Fig. 2. **2D-NOESY spectrum of calix[4]arene C-145F**

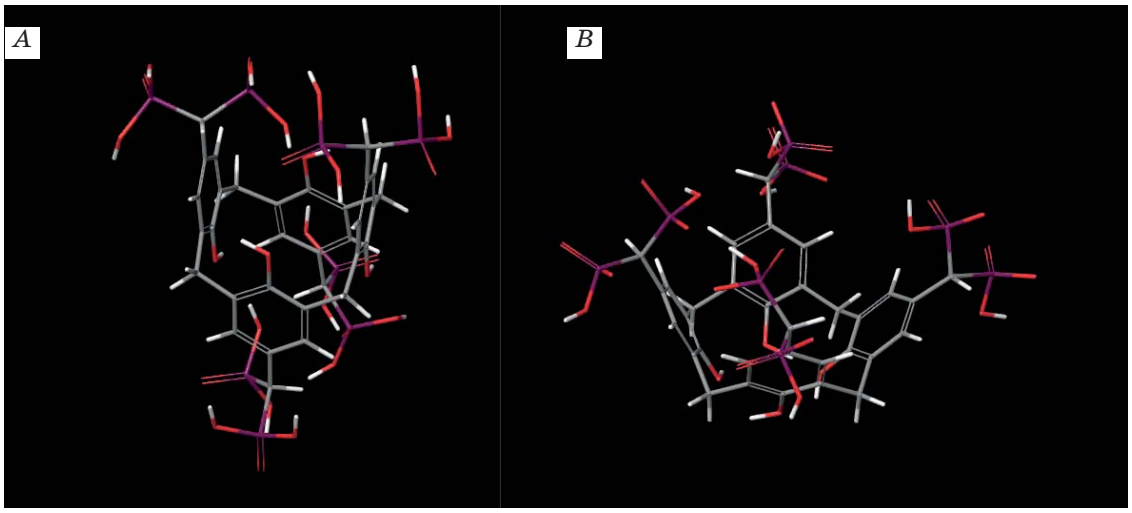

Fig. 3. **Structure of calix[4]arene C-145 and it's analogue with fixed conformation of a calix[4]arene cup:**
A — C145; *B* — C145F

Results. Using a 2D NMR-NOESY spectroscopy, we can observe a distinct cross-peak between an aromatic singlet with a chemical shift on 7.72 ppm and protons of isopropyl group with a chemical shift on 1.62 ppm, which are moved in the strong field (Fig. 2). This correlation proves us their steric proximity, that can be observed only in conus-conformation (Fig. 3, *A*), not in the *1,3-alternat*e. So, in this work we confirmed that disubstituted calix[4]arenes (low-rim modification) have fixed conus conformation.

NMR spectroscopy proves us that calix[4]arene C145F exists in fixed conus-conformation.

Discussion. Presented experiment represents how easily we can modify calix[4]arene cup in order to obtain molecule with new chemical and physical properties. The fine-tuning and incorporation of different ligating sites in the calix[4]arene scaffold may be used to produce numerous molecules, forming a library of compounds.

Comparison of the action of fibrin polymerization of calix[4]arene molecules with fixed and opened conformations will allow to estimate the role of different conformation in fibrin recognition and will support targeted design of even more effective calix[4]arene-based inhibitors of blood clotting in future.

Conclusions. The easy method of the fixation of conus conformation of calix[4]arene cup will be useful for synthesis of novel functionally active compounds. We believe that further development and study of different calix[4]arenes will help scientists to obtain bioactive molecules that could be prospective anti-thrombotic drugs.

Key words: calix[4]arene; fibrin polymerization; organic synthesis;, bioinformatics.

Acknowledgement. Authors gratefully acknowledge Prof. V. I. Kalchenko, Dr. V. O. Chernysheko, and Dr S. O. Cherenok for their contribution to this work.

Author's contribution. DA performed synthesis of calix[4]arenes, OH did molecular modeling.

Funding source. The research was financed by the project 0119U002512: "The interaction of the hemostasis system components at the cellular and molecular level in the process of formation and elimination of a thrombus".

REFERENCES

1. *Aaron M. Wendelboe, Gary E. Raskob* (2016). Global Burden of Thrombosis Epidemiologic Aspects. Circulation Research 118(9), 1340-1347. https://doi.org/10.1161/CIRCRESAHA.115.306841
2. *SIXTY-SIXTH WORLD HEALTH ASSEMBLY*. A/RES/66/2. 27 May 2013

3. *Rajesh Kumar, Amit Sharma, Hardev Singh, Paolo Suating, Hyeong Seok Kim, Kyoung Sunwoo, Inseob Shim, Bruce C. Gibb and Jong Seung Kim*. Revisiting Fluorescent Calixarenes: From Molecular Sensors to Smart Materials. *Chem. Rev.* 2019, 119(16), 9657–9721. https://doi.org/10.1021/acs.chemrev.8b00605
4. *Didkivskyi V., Pavlenko A.* Aprobation of calix[4]arene C-145 as antitrombotic agent *in vivo*. *Biotechnologia acta*. 2022, 15(5), 41–46. https://doi.org/10.15407/biotech15.05.041
5. *Didkivskyi V.A., Pavlenko A.O., Marunych R.Y., Selikhova A.O., Cherenok S.O., T.P. Todosiuk., Shevchenko S.M*. HPLC detection of antithrombitic calix[4]arene in blood plasma of animals. *Biotechnologia Acta* 2022, 15(2), 51–52. https://doi.org/10.15407/biotech15.02.051
6. *Lugovskoy E.V., Gritsenko P.G., Koshel T.A., Koliesnik I.O., Cherenok S.O., Kalchenko O.I., Kalchenko V.I., Komisarenko S.V*. Calix[4]arene methylenebisphosphonic acids as inhibitors of fibrin polymerization. *FEBS J*. 2011, 278(8), 1244–1251. https://doi.org/10.1111/j.1742-4658.2011.08045.x

UDC 577.2 **https://doi.org/10.15407/biotech16.02.011**

FIBRINOGEN-SPECIFIC PROTEASE IN THE *Vipera renardi* SNAKE VENOM

K. V. BAIDAKOVA[1, 2], *Y. M. STOHNII*[2], *O. M. PLATONOV*[2]

[1]Educational and Scientific Center "Institute of Biology and Medicine"
of Taras Shevchenko National University of Kyiv, Ukraine
[2]Palladin Institute of Biochemistry
of the National Academy of Sciences of Ukraine, Kyiv

E-mail: katrinbaidakova@gmail.com

Received 2023/03/23
Revised 2023/04/12
Accepted 2023/04/28

Venoms of snakes of Viperidae family contain the mixtures of physiologically active proteins. Evolutionary they were developed for the effective envenomation of the prey, however, their high specificity towards components of mammal blood makes them a prospective pharmacological agent [1]. Some of these enzymes are targeted preferentially to fibrinogen [1–3]. Fibrinogen-specific proteases of snake venoms are assumed as a possible agent for defibrin(ogen)ation and the achieving of antithrombotic effect. Also, their application is one of the possible approaches for studying structure and functions of fibrinogen molecule. That is why the aim of the present study was the search of fibrinogenolytic enzymes among protein components of *Vipera renardi* snake venom.

Methods. Venom of *V. renardi* as the lyophilized powder was supplied by Trypillia serpentarium. It was dissolved in 0.05 M Tris-HCl buffer pH 8.3 and fractionated on Superdex G-75 using FPLC system Acta Prime. Peaks were tested for their ability to directly cleave fibrinogen. For this, the fraction with the lowest light absorption at 280 nm was diluted 5 times and fibrinogen was added to its final concentration of 2 mg/ml. Other peaks were diluted an appropriate number of times so that all fractions were commensurate. Incubation continued for 2 hours at a temperature of 37 °C. Hydrolytic products were analyzed by SDS-PAGE. Enzyme-electrophoresis with fibrinogen co-polymerized in 12% polyacrylamide gel was used for the identification of protein that can cleave fibrinogen.

Results. Venom of *V. renardi* was fractionated on 4 fractions using size-exclusion chromatography. SDS-PAGE of fibrinogen hydrolysis products showed the presence of fibrinogen-specific protease in the 1st and 2nd fractions of venom. 2nd fraction was much more active and according to the data of enzyme electrophoresis contained protease with molecular mass 25 kDa.

Discussion. Fibrinogen is a large blood plasma glycoprotein. When blood vessels are damaged, a cascade of reactions is triggered, the final result of which is the transformation of fibrinogen into fibrin, which polymerizes to form the core of a blood clot that terminates bleeding [4]. However, certain pathological conditions increase the risk of intravascular blood clotting which affect the normal blood supply of tissues and can be a deadly threat. Therefore, the search for proteases targeted fibrinogen and fibrin can be assumed as agents for direct defibrination [5]. The protease found in the present study effectively cleaves fibrinogen and can be tested for its ability to act on blood clots in the bloodstream.

Proteases that exhibit fibrinogenolytic activity can also be tools for studying of the structure and function of fibrin(ogen) molecule. Under the action of fibrinogenolytic enzymes we can obtain fragments of the molecule which study can indicate the role of different sites in the functioning of fibrinogen [6]. Therefore, the next stage of the study of the obtained protease will be the detection of the hydrolysis point within the fibrinogen molecule, which will allow obtaining unique proteolytic fragments.

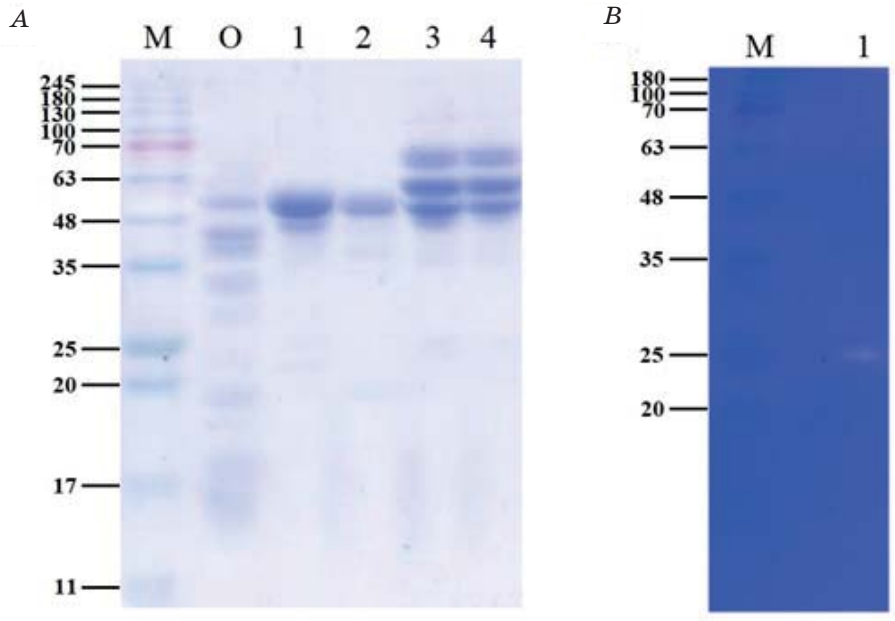

SDS-PAGE of fibrinogen hydrolysis products by fractions obtained using Superdex G-75 (*A*):
M —markers, kDa; O — venom of V. renardi; 1–4 —studied samples.
Enzyme-electrophoresis with fibrinogen co-polymerized in 12% polyacrylamide gel of fraction with fibrinogenolytic activity of Vipera renardi snake venom (*B*):
M — markers, kDa; 1 — studied sample

Conclusions. Fractionation of *V. renardi* snake venom allowed to detect a protease with apparent molecular mass 25 kDa that can cleave fibrinogen molecule.

Key-words: proteases; fibrinogen; snake venom; vipera.

Acknowledgement. Authors gratefully acknowledged Dr Chernyshenko for his encouragement of these studies.

Authors' contribution. KB and OP fractionated venom of *V. renardi*. KB and YS studied the ability of obtained fractions to cleave fibrinogen.

Funding source. The research was financed by the project 0119U002512: "The interaction of the hemostasis system components at the cellular and molecular level in the process of formation and elimination of a thrombus."

REFERENCES

1. *Frangieh J., Rima M., Fajloun Z., Henrion D., Sabatier J., Legros C., Mattei C.* Snake venom components: tools and cures to target cardiovascular diseases. *Molecules*. 2021, 26(8), 2223. https://doi.org/10.3390/molecules26082223
2. *Kini R. M.* Anticoagulant proteins from snake venoms: structure, function and mechanism. *The Biochemical journal*. 2006, 397(3), 377–387. https://doi.org/10.1042/BJ20060302
3. *Cortelazzo A., Guerranti R., Bini L., Hope-Onyekwere N., Muzzi C., Leoncini R., Pagani R.* Effects of snake venom proteases on human fibrinogen chains. *Blood Transfus*. 2010, 8(3), 120–125. https://doi.org/10.2450/2010.019S
4. *Weisel J. W., Litvinov R. I.* Fibrin Formation, Structure and Properties, *Subcell Biochem*. 2017, 82, 405–456. https://doi.org/10.1007/978-3-319-49674-0_13
5. *Markland F. S., Swenson S.* Fibrolase: trials and tribulation. *Toxins (Basel)*. 2010, 2(4), 793–808. https://doi.org/10.3390/toxins2040793
6. *Stohnii Y. M., Yatsenko T. A., Nikulina V. V., Kucheriavyi Y. P., Slominskyi O. Yu., Savchenko K. S., Garmanchuk L. V., Varbanets L. D., Tykhomyrov A. O., Chernyshenko V. O.* Functional properties of individual sub-domains of the fibrin(ogen) αC-domain. *BBA Advances*. 2023, 3, 100072. https://doi.org/10.1016/j.bbadva.2023.100072

UDC 577.218+616-006 https://doi.org/10.15407/biotech16.02.013

OVEREXPRESSION/KNOCKDOWN OF ADAPTOR PROTEIN RUK/CIN85 IN HUMAN LUNG ADENOCARCINOMA A549 CELLS RESULTS IN OPPOSITE CHANGES BETWEEN MMP-2/MMP-9 EXPRESSION LEVELS/ACTIVITIES AND CELL`S INVASION

M. I. BEKALA[1,2], *D. S. GERASCHENKO*[1], *O. V. KHUDIAKOVA*[1], *T. D. SKATERNA*[1]

[1]Palladin Institute of Biochemistry of NAS of Ukraine, Kyiv
[2]Taras Shevchenko National University, Kyiv, Ukraine

E-mail: markbekala2@gmail.com

Received 2023/03/16
Revised 2023/04/14
Accepted 2023/04/28

To acquire the ability to metastasize, cancer cells undergo molecular reprogramming in the course of epithelial-mesenchymal transition resulting in an increased motility and invasiveness [1]. Cells with elongated spindle-like mesenchymal phenotype require ECM-degrading enzymes, mainly MMP-2 and MMP-9, to generate the path for migration. In our previous works we demonstrated that overexpression of adaptor protein Ruk/CIN85 in breast cancer cells was associated with their aggressive metastatic behavior [2, 3]. In this study we aimed to investigate the changes in MMPs expression and activity as well as invasiveness of human lung adenocarcinoma A549 cells with up-/down-regulation of Ruk/CIN85.

Methods. We used A549 cells with stable overexpression (subline RukUp) and knockdown of Ruk/CIN85 (subline RukDown), as well as corresponding vector control sublines Mock and Scr.

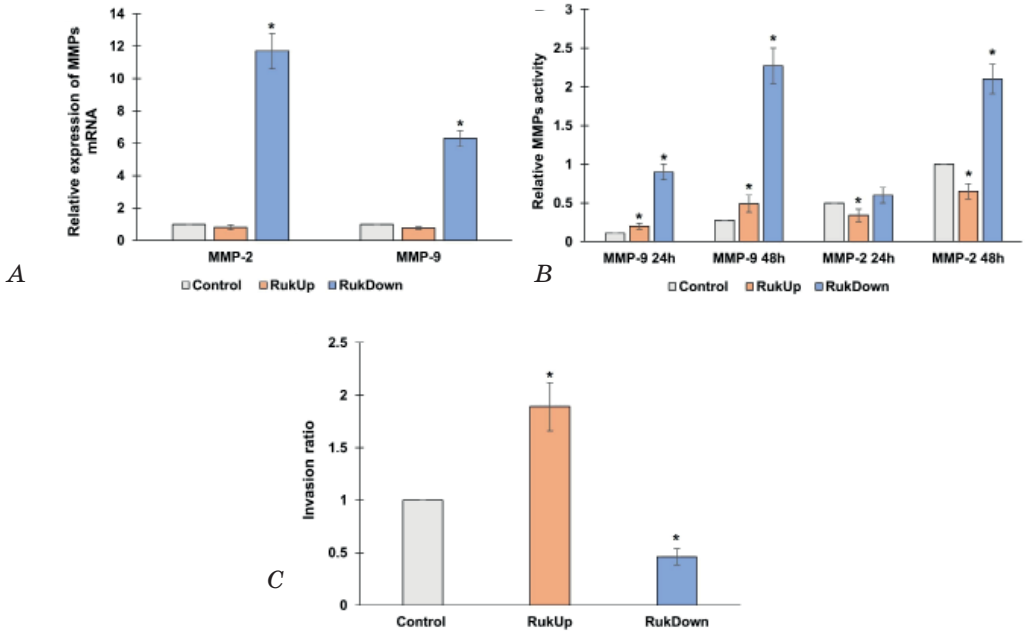

Fig. **Up-/down-regulation of Ruk/CIN85 in human lung adenocarcinoma A549 cells lead to opposite changes between MMP2/MMP9 genes expression (*A*); their enzymatic activities (*B*) and invasion ratio of cell sublines (*C*):**
$M \pm m$, $n = 3$; * — $P < 0.05$ compared to the corresponding control

Cells were cultured in the complete DMEM medium under standard conditions. mRNA expression levels were estimated by RT^2-PCR, enzymatic activity was assessed using gelatin zymography. Invasiveness of cancer cells was studied using Boyden chambers coated with Matrigel.

Results. Analysis of mRNA expression of MMPs in RukUp and RukDown cells revealed that MMP-2 and MMP-9 were preferentially overexpressed in RukDown cells, while RukUp subline did not exhibit significant difference compared with corresponding control (Fig. *A*). These findings were confirmed and complemented by study of enzyme activities. As can be seen from Fig. ***B***, the gelatinolytic activities of both MMP-2 and MMP-9 were dramatically increased in RukDown subline, compared to respective control (Fig. *B*). Surprisingly, we revealed that MMPs regulation was inversely correlated with invasion potential of Ruk/CIN85 up/down A549 cells. In particular, it was established that invasiveness of RukUp cells was 2 times higher in comparison with respective control subline. Alternatively, invasion ratio was significantly decreased in RukDown cells (0.5 times) in comparison with control (Fig. *C*).

Discussion. In this study we found that expression level of Ruk/CIN85 in A549 cells is strongly associated with opposite changes between their invasiveness and MMPs expression/activities. It is known that the role of MMPs in carcinogenesis remains ambiguous. MMPs are involved in tumor progression. In particular, MMP`s associated degradation of ECM components modulates cancer cells motility as well as leads to activation of proangiogenic factors in various cancerous tissues. On the other hand, MMP-2/MMP-9 take part in digestion of plasminogen resulting in generation of angiostatins (kringle–containing fragments of plasminogen) that could function as inhibitors of angiogenesis and tumor growth *in vitro* and *in vivo* [4].

Conclusions. According to the data received, it is possible to suggest that up-regulation of adaptor protein Ruk/CIN85 in A549 cells can lead to the very aggressive MMP-independent mode of migration that rely on cycles of expansion and contraction of the cell body mediated by the cortically localized actin and myosin [5].

Key words: Lung Adenocarcinoma; Motility; Invasion; Epithelial-Mesenchymal Transition; MMPs; Adaptor Protein Ruk/CIN85.

Author`s contribution. Bekala M. I. has performed estimation of mRNA expression levels by RT^2-PCR as well as was involved in zymography assay, data analysis and thesis writing. Geraschenko D. S. has received sublines of A549 cells with stable expression and knockdown of Ruk/CIN85. Khudiakova O. V. worked on the RNA extraction. Skaterna T. D. has performed zymography and Boyden chamber assays, as well as has curated research planning, data analysis and thesis writing.

Acknowledgments. We express our gratitude to Professor Liudmyla Drobot for scientific guidance and support of our work.

REFERENCES

1. *Stuelten C. H., Parent C. A., Montell D. J.* Cell motility in cancer invasion and metastasis: insights from simple model organisms. *Nat Rev Cancer*. 2018, 18(5), 296–312. https://doi.org/10.1038/nrc.2018.15
2. *Samoylenko A., Vynnytska-Myronovska B., Byts N., Kozlova N., Basaraba O., Pasichnyk G., Palyvod K., Bobak Y., Barska M., Mayevska O., Rzhepetsky Yu., Shuvayeva H., Lyzogubov V, Usnko V., Savran V., Volodki N. Buchman V., Kietzmas T., Drobot L.* Increased levels of the HER1 adaptor protein Rukl/CIN85 contribute to breast cancer malignancy. *Carcinogenesis*. 2012, v. 33, 1976–1984. https://doi.org/10.1093/carcin/bgs228
3. *Horak I., Drobot L., Borsig L., Knopfova L., Smarda J.* Overexpression of adaptor protein Ruk/CIN85 in mouse breast adenocarcinoma 4T1 cells induces an increased migration rate and invasion potential. *Biopolymers and Cell*. 2018, 34 (4), 284–291. https://doi.org/10.7124/bc.000981
4. *Merchant N., Nagaraju G.P., Rajitha B., Lammata S., Jella K.K., Buchwald S., Lakka S., Ali.A.N.* Matrix metalloproteinases: their functional role in lung cancer. *Carcinogenesis*. 2017, 38(8), 766–780. https://doi.org/10.1093/carcin/bgx063
5. *Panková K., Rösel D., Novotný M., and Brábek J.* The molecular mechanisms of transition between mesenchymal and amoeboid invasiveness in tumor cells. *CMLS*. 2010, v. *67*, 63–71. https://doi.org/10.1007/s00018-009-0132-1

UDC 577.218+577.214.6+615.322+59.084

https://doi.org/10.15407/biotech16.02.015

Rhodiola rosea AND FERULIC ACID ACTIVATE EXPRESSION OF GENES RELATED TO AUTOPHAGY AND RESISTANCE TO HEAT SHOCK IN MICE OF DIFFERENT AGE

O. I. DEMIANCHUK, M. V. IVANOCHKO, D. V. GOSPODARYOV, M. M. BAYLIAK

Department of Biochemistry and Biotechnology
of Vasyl Stefanyk Precarpathian National University, Ivano-Frankivsk, Ukraine

E-mail: oleh.demianchuk@pnu.edu.ua

Received 2023/03/28
Revised 2023/04/19
Accepted 2023/04/28

Rhodiola rosea is a medicinal plant, whose extracts extend lifespan of many animals. Ferulic acid, one of the active components of *R. rosea*, has recently been shown to prolong lifespan in the nematode *Caenorhabditis elegans* model [1]. Several studies have shown that active components of *R. rosea* activate transcription factor FoxO (forkhead box O) [2, 3]. In turn, FoxO regulates expression of genes encoding heat shock proteins, proteins involved in genome repair, autophagy, and antioxidant defence, etc. Also, many anti-aging preparations were shown to activate autophagy [4].

The aim of our study was testing whether *R. rosea* extract and ferulic acid activate expression of targets of FoxO, regulators of energy metabolism and autophagy in livers of young and old mice, and to what extent the effects of *R. rosea* extract and ferulic acid on the genes studied coincide.

Methods. C57BL/6J mice were reared at 22 ± 2 °C, 50–60% humidity, and 12/12 hour light/dark cycle. All groups were reared on a standard chow (4.8% fats, 21.8% protein, and 3.9% fibre). Experimental groups consumed water, supplemented with either sodium ferulate or *R. rosea* during 12 weeks prior sacrificing. The amounts of ferulate and *R. rosea* were adjusted to provide 4 mg of phenol-containing substances per 100 g weight, for a mouse, for 24 hours. We tested three-month-old ("young") and twelve-month-old males ("old").

The levels of messenger ribonucleic acid (mRNA) were assessed using AriaMx real-time polymerase chain reaction (RT-PCR) instrument (Agilent). Ribonucleic acid was purified using the Monarch Miniprep kit (New England BioLabs (NEB), T2010), complementary deoxyribonucleic acid synthesis was performed using the ProtoScript II kit (NEB, E6560), and quantitative RT-PCR (qRT-PCR) was performed using the Luna Universal kit (NEB, E3003). The expression of genes ATG5 (an autophagy marker), HSPB8 (a small heat shock protein, an FoxO target), UCP2 (uncoupling protein 2, a senescence marker), CDKN2 (cell cycle regulator, a senescence marker), PDK2 and PDK4 (pyruvate dehydrogenase kinases 2 and 4, regulators of oxidative metabolism), and TFEB (transcription factor EB, a transcriptional regulator of autophagy) was evaluated.

Results. Livers of young mice that consumed food supplemented with either sodium ferulate or *R. rosea* extract had 3.2-fold and 3.6-fold higher levels of mRNA of the small heat shock protein HspB8 than control mice, respectively (Fig. 1).

In old mice, the levels of mRNA for this protein were 3.3-fold higher in mice reared on the diet containing *R. rosea* extract as compared with the control (Fig. 2). However, there was no significant difference between control mice and those that consumed ferulate-supplemented food (Fig. 2).

In young mice, ferulate and *R. rosea* extract induced synthesis of mRNA of PDK4 by 4.3 and 6.6 times from the control level, respectively (Fig. 1). The difference in the levels of mRNA for PDK4 between control and experimental groups did not extinguish with age since old mice fed with ferulate and *R. rosea* supplemented food had 5.6- and 6.3-fold higher levels of mRNA for PDK4 as compared with the control (Fig. 2). Ferulate and *R. rosea* extract also affected the levels of mRNA of ATG5 and PDK2 in the livers of old mice. In particular, the levels of mRNA of ATG5 were 2.6- and 2.8-

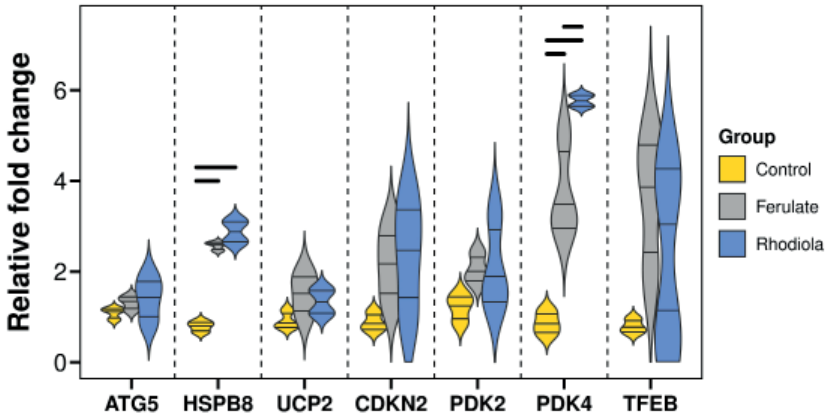

Fig. 1. **Relative levels of mRNA of the genes studied in the livers of three-month-old mice consuming food with or without sodium ferulate or *R. rosea* extract:**
horizontal bars denote statistically significant differences (Duncan's test, $P < 0.05$, $n = 3$)

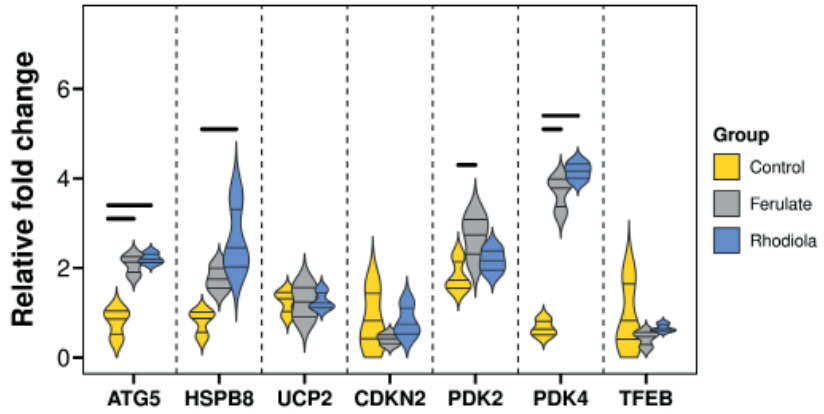

Fig. 2. **Relative levels of mRNA of the genes studied in the livers of twelve-month-old mice consuming food with or without sodium ferulate or *R. rosea* extract:**
horizontal bars denote statistically significant differences (Duncan's test, $P < 0.05$, $n = 3$)

fold higher in old mice consumed ferulate- and *R. rosea* supplemented food, respectively, as compared with the control. The levels of PDK2 were 1.5-fold higher in the livers of mice that consumed ferulate-supplemented food than in control mice.

Discussion. *R. rosea* preparations were shown to increase expression of small heat shock proteins [3]. This is confirmed by our current data. In addition, we have shown that *R. rosea* and ferulic acid may suppress generation of adenosine triphosphate (ATP) in the oxidative phosphorylation by increasing expression of PDK2 and PDK4. In turn, PDK2 and PDK4 inhibit pyruvate dehydrogenase complex (PDC). The inhibition of PDC blocks entry of pyruvate into the tricarboxylic acid cycle (TCA). Consequently, it suppresses production of reducing equivalents required for the operation of oxidative phosphorylation. Decrease in production of ATP leads to concomitant increase in the levels of adenosine monophosphate, a well-known inducer of autophagy [4]. Activation of autophagy markers, such as ATG5, we observed in the livers of old mice reared on the food with ferulate and *R. rosea*.

Our data identify a set of molecular targets that may account for the adaptogenic and anti-aging properties of ferulic acid and *R. rosea*. In addition, we have shown that *R. rosea* and ferulic acid treatments do not affect such well-known markers of aging as CDKN2, and do not influence autophagy via TFEB.

Conclusions. Both, *R. rosea* extract and one of its active components — ferulic acid — promote increasing in the levels of mRNA for genes HSPB8 and PDK4, coding for small heat shock protein and pyruvate dehydrogenase kinase 4, respectively. In old mice, *R. rosea* promote expression of HSPB8, ATG5, PDK2, and PDK4. Thus, ferulic acid and *R. rosea* exert

similar effects on gene expression by supposed activation of heat shock response and autophagy, and concomitant inhibition of mitochondrial metabolism via boosting expression of PDK2 and PDK4.

Key words: Rhodiola rosea; ferulic acid; mice; PDK4; autophagy; mRNA.

Acknowledgement. Authors acknowledge Dr. Maria Lylyk, Ihor Yurkevych and Halyna Shmihel for the assistance with purchasing reagents and equipment, company BioLabTech, LTD for the excellent client service, Nadia Stefanyshyn, and bachelor and master students that conduct their research at our department for their assistance at multiple stages of measurement.

Authors' contribution. OID composed the diets and assisted in qRT-PCR, MVI carried about the animals and assisted in qRT-PCR, DVG conducted qRT-PCR and wrote the abstract, MMB conceived and designed the study, and provided resources for the work.

Funding source. This research was supported by the grant #2020.02/0118 from the National Research Foundation of Ukraine to MMB.

REFERENCES

1. *Li H., Yu X., Meng F., Zhao Z., Guan S., Wang L.* Ferulic acid supplementation increases lifespan and stress resistance via insulin/IGF-1 signaling pathway in *C. elegans*. *Int. J. Mol. Sci.* 2021, 22 (8), 4279. https://doi.org/10.3390/ijms22084279
2. *Jiang S., Deng N., Zheng B., Li T., Liu R. H. Rhodiola* extract promotes longevity and stress resistance of *Caenorhabditis elegans* via DAF-16 and SKN-1. *Food. Funct*. 2021, 12 (10), 4471–4483. https://doi.org/10.1039/d0fo02974b
3. *Wiegant F. A., Surinova S., Ytsma E., Langelaar-Makkinje M., Wikman G., Post J. A.* Plant adaptogens increase lifespan and stress resistance in *C. elegans*. *Biogerontology*. 2009, 10 (1), 27–42. https://doi.org/10.1007/s10522-008-9151-9
4. *Liu J. K.* Antiaging agents: safe interventions to slow aging and healthy life span extension. *Nat. Prod. Bioprospect*. 2022, 12 (1), 18. https://doi.org/10.1007/s13659-022-00339-y

UDC 576.3(075.8) **https://doi.org/10.15407/biotech16.02.018**

THE EFFECT OF BROCCOLI SPROUTS ON OXIDATIVE STRESS MARKERS IN MICE FED WITH CAFETERIA DIET

V. P. DERKACHOV, M. V. IVANOCHKO, M. M. BAYLIAK

Vasyl Stefanyk Precarpathian National University
Department of Biochemistry and Biotechnology Ivano-Frankivsk, Ukraine

E-mail: derkachovvitalii@gmail.com

Received 2023/02/28
Revised 2023/04/08
Accepted 2023/04/28

In recent years, growing interest has been shown in the health advantages of broccoli sprouts [5]. These juvenile plants, which are taken just a few days after germination, contain bioactive substances that have been proven to offer a variety of health benefits. Sulforaphane has attracted the most interest among these substances because of its powerful anti-cancer properties [2]. Studies indicate that in addition to possibly protection against cancer, cardiovascular disease, diabetes, and neurological diseases, broccoli sprouts may also have other health advantages [1]. The anti-inflammatory effects of broccoli sprouts are thought to be mediated by several mechanisms. Sulforaphane has been shown to inhibit the activation of NF-kB, a key regulator of the inflammatory response, while glucoraphanin has been shown to enhance the production of anti-inflammatory compounds such as interleukin-10 [4]. Kaempferol, another bioactive compound found in broccoli sprouts, has been shown to inhibit the production of inflammatory cytokines [3]. Anti-inflammatory properties of broccoli sprouts may help to attend inflammation-related oxidative stress that may be beneficial for preventing and treating a range of diseases associated with development of both inflammation and oxidative stress, in particular diet-associated obesity [6]. Therefore, the aim of our study was to determine the ability of broccoli sprouts to influence the intensity of lipid peroxidation in mice fed a high-calorie cafeteria diet [7].

Materials and Methods. In this study, C57BL/6J mice were used. Mice were divided in 4 groups. The first group was the control group and was fed with a standard food. The second group was fed with a standard food with the addition of broccoli sprouts (broccoli group). Mice of the third group fed with a cafeteria diet, which consisted of 70% cafeteria food and 30% standard food (cafeteria diet group). The fourth group was fed with a cafeteria diet with the addition of broccoli sprouts (5% by weight). At the beginning of the experiment, the mice were 9 months old. The experiment lasted 4 months. During experiment body mass of mice was monitored.

In the end of the experiment, the mice were euthanased and organs were harvested to determine the intensity of lipid peroxidation. The frozen tissues were homogenised in 96% ethanol at a ratio of 1:10, centrifugired for 10 min at 10,000 rpm, and supernatants were collected. For determinatiom of lipid peroxides (LOOH), we used a method based on the ability of lipid peroxides to convert Fe^{2+} to Fe^{3+}. Then Fe^{3+} forms a complex with xylenol orange that absorbs light at 580 nm at low pH. The reaction mixture contained coumene hydroperoxide (1 mM), $FeSO_4*7H_2O$(1 M), xylenol (4 mM), water and supernatant. Differences between groups were analyzed by Duncan's test for multiple comparision.

Results and Discussion. During the experiment, we monitored the changes in body mass of mice fed with different diets and results are presented in Fig. 1.

Next, we measured levels of LOOH in cortex, hypothalamus and muscles for understanding whether inflammatory and oxidative processes have begun. As we can see in Fig. 2, *A*, there was no differences in LOOH levels in cortexes of mice from all experimental groups, but there was a tendency to the lower content of LOOH in the brain of mice fed with cafeteria diet and broccoli.

Then, we decided to measure LOOH in hypothalamus (*B*) as an organ vulnerable for inflammation. No statistical differences in levels of LOOH were found between groups, but LOOH levels tended to the highest in the groups fed with broccoli sprouts alone and cafeteria diet.

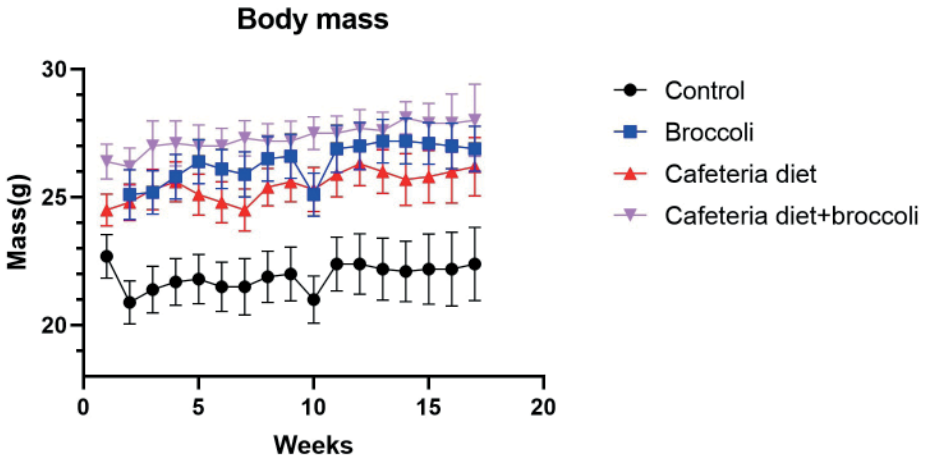

Fig. 1. **Body mass of mice fed with different diets, $n = 7–8$**

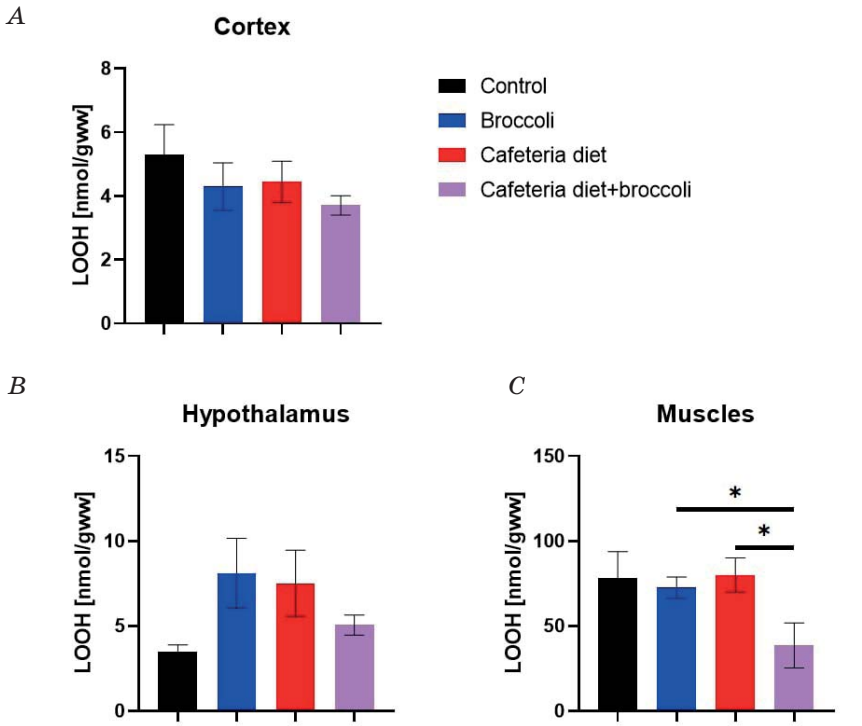

Fig. 2. **Level of LOOH in cortex(*A*), hypothalamus (*B*), muscles (*C*)** ***n*** =7–8. Used Dunkan's test.

A significant difference was observed in the muscles (*C*) between the broccoli sprout group and the cafeteria diet + broccoli group. We also found a significant difference between the group fed with the cafeteria diet and the cafeteria diet + broccoli, which may indicate protective effects of broccoli on lipid peroxidation on cafeteria diet.

Conclusions

1. Mice fed with cafeteria diet and broccoli spouts had higher body mass than control mice fed with standard group.

2. Hypothalamus of mice fed with standard diet with broccoli spouts or with cafeteria diet showed a tendency to higher LOOH levels, whereas no effects of the diets were found on cortexes LOOH levels.

3. The cafeteria diet + broccoli group had the lowest muscle LOOH content compared to all other groups. Also, LOOH levels tended to be lower in the cortexes in the hypothalamus of mice fed with cafeteria diet + broccoli as compared with the cafeteria diet group. This suggests the potential protective effects of broccoli spouts.

Keywords: broccoli; lipid peroxides; inflammation.

Authors' contribution. V. P. Derkachov — Investigation, Data analysis; M. M. Bayliak — supervisor, M. V. Ivanochko helping with measurements; Volodymyr I. Lushchak: funding acquisition, design of the study.

Funding. This work was supported by a grant from Ministry of Education and Science of Ukraine for VIL (#0122U000894).

REFERENCES

1. *Egner P. A., Chen J. G., Zarth A. T., Ng D. K., Wang J. B., et al.* Rapid and sustainable detoxication of airborne pollutants by broccoli sprout beverage: results of a randomized clinical trial in China. *Cancer prevention research (Philadelphia, Pa.)*. 2014, 7(8), 813–823. https://doi.org/10.1158/1940-6207.CAPR-14-0103
2. *Heber D., Li Z., Garcia-Lloret M., Wong A. M., Lee T. Y., Thames G., Krak M., Zhang Y., Nel, A.* Sulforaphane-rich broccoli sprout extract attenuates nasal allergic response to diesel exhaust particles. *Food & function*. 2014, *5*(1), 35–41. https://doi.org/10.1039/c3fo60277j
3. *Kim H, Kim E, Choe J.* Sulforaphane inhibits the activation of inflammatory response in human primary synovial cells. *Food Sci Biotechnol.* 2021, 30(3). 419–427. https://doi.org/10.1007/s10068-020-00851-2
4. *Kim H, Kim E, Park S, Kim J, Kim H.* Sulforaphane regulates the expression of Th1/Th2 cytokines and chemokines via the Nrf2/ARE pathway in mouse bone marrow-derived macrophages. *Food Sci Biotechnol.* 2018, 27(6), 1703–1710. https://doi.org/10.1007/s10068-018-0441-9
5. *Kong F, Zhang J, Li Y.* Protective effect of sulforaphane against skeletal muscle injury induced by ischemia-reperfusion through regulation of mitochondrial fusion/fission. *Food Funct.* 2021, 12(1), 79–88. https://doi.org/10.1039/d0fo02255a
6. *Talalay P, Fahey JW.* Phytochemicals from cruciferous plants protect against cancer by modulating carcinogen metabolism. *J Nutr.* 2001, 131(11 Suppl), 3027S–3033S. https://doi.org/10.1093/jn/131.11.3027S
7. *Xiao D, Liu C, Li J.* Sulforaphane attenuates microglia-mediated neuroinflammation and enhances microglial autophagy via the Nrf2/ARE pathway. *Aging (Albany NY).* 2021, 13(1), 358–374. https://doi.org/10.18632/aging.202184

UDC 577.2 **https://doi.org/10.15407/biotech16.02.021**

DETECTION OF TERNARY COMPLEX OF FIBRIN DESAB WITH D-DIMER AND D-FRAGMENT OF FIBRIN

O. HRABOVSKYI[1], *M. SYRKO*[1, 2]

[1] Palladin Institute of biochemistry the National Academy of Sciences of Ukraine, Kyiv
[2] Educational and Scientific Center "Institute of Biology and Medicine"

E-mail: grabalexey@gmail.com

Received 2023/04/12
Revised 2023/04/21
Accepted 2023/04/28

Introduction. The fibrinogen molecule is a key protein in the haemostasis system, which is converted by thrombin into fibrin that polymerizes and forms a highly complex supramolecular structure [1]. This is done by stepwise cleavage of pairs of fibrinopeptides A (16 amino acid residues at the N-termini of the Aα chains) and fibrinopeptides B (14 amino acid residues at the N-termini of the Bβ chains) by thrombin, as a result, polymerization sites "A" and "B" are exposed on the fibrin molecule, while the complementary sites "a" and "b" that are located in the γ- and β-nodules are preexisted in the fibrinogen molecule [2].

The interaction of these sites, primarily "A:a", leads to the formation of a protofibril, which can be considered the first stage of fibrin polymerization. The second stage which is the lateral association of protofibrils is driven by the interaction of "B:b" polymerization sites, αC-regions of fibrin molecules and the interaction of D-regions of fibrin molecules that belongs to the neighbouring protofibrils [1, 3, 4].

Model systems are one of the approaches to study the mechanism of fibrin self-assembly. Experimental data obtained on such models can be used to elucidate the mechanisms of interaction of individual functional domains of fibrin molecules and characterize the polymerization process in general. Therefore, the aim of this work is to study the intermolecular interactions of fibrin with D-domain-containing fragments of fibrin(ogen): D-dimer and D-fragment.

Methods. Human fibrinogen was obtained from the human blood plasma by salt extraction using 16 % Na_2SO_4. The content of protein coagulated by thrombin — 96–98%. The precipitated fibrinogen was diluted in 0.15 M NaCl, the solution was frozen and stored with −20 °C [5]. Fibrin desAB was obtained by thrombin action on fibrinogen with following dissolving in 0.125 % acetic acid. D-dimer and D-fragment of fibrin were obtained by plasmin hydrolysis of cross-linked fibrin desAB or fibrinogen respectively with following purification using size-exclusion chromatography on Sephacryl S-300 HR and characterized by SDS-PAGE.

Analytical size-exclusion chromatography for the detection of molecular complexes was performed on the Sepharose 6B column (30×0.5 cm). Components of the analyzed mixture (0.8 ml) were separated by standard chromatography protocol: speed of elution — 0.5 ml/min; collected samples volume —0.5 ml. Optical density of collected samples was measured by spectrophotometer POP (Optizen, Daejeon, Korea). Composition of each sample was analyzed by SDS-PAGE. Relative amounts of studied compounds in samples were analyzed using densitometry of scanned electropherograms with Totallab TL100 software [6].

Molecular modeling of complexes formed by fibrin desAB and its fragments were performed using UCSF Chimera 1.16 on the basis on earlier developed protofibril structure [7]. This structure was prepared for molecular docking by removing and truncating all chains except those belonging to the sole molecule of fibrin and corresponding D-dimer, adding hydrogens with subsequent energy minimization of the complex. The structure of the D-region (PDB ID:1LTJ) was prepared in the same way. The protein-protein molecular docking was performed using HDOCK web server [8].

Results. To investigate the complex formation between fibrin desAB (fibrin with both cleaved fibrinopeptides A and B) and its degradation products, we used size-exclusion chromatography,

which allows separating different fractions of proteins depending on their molecular weight. It also can be an option for evaluation if larger, high-affinity protein-protein complex is formed [9].

To verify and calibrate the retention volume of the mixture components: fibrin monomer and fibrin(ogen) fragments, each component was applied to the column separately. The fibrin exit zone corresponded to a volume of 7 ml, D-dimer to 8 ml, and D-fragment to 9.5 ml.

To obtain the fibrin-DD-D complex we have composed a mixture of fibrin desAB (1 mg/ml) with D-dimer and D fragment in the molar ratio 0.8:1:1. Fragments were added to the 0.05 M Tris-HCl buffer pH 7.4 with 0.4 M NaCl and 0.001 M $CaCl_2$. Monomeric fibrin desAB dissolved in 0.125 % acetic acid was added to the solution of fragments in a small volume. The mixture was applied to the Sepharose 6B column after 30 min of incubation at ambient temperature. The elution profiles were monitored and the composition of obtained fractions were analyzed by SDS-PAGE. The formation of a stable ternary complex «desAB-DD-D» was observed using SDS-PAGE (Fig. 1).

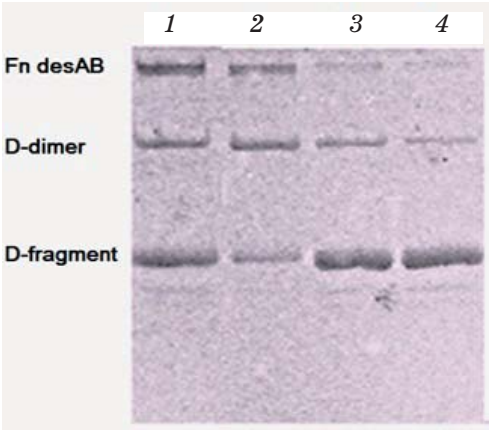

Fig. 1. **SDS-PAGE of fractions eluted from the Sepharose 6B column:**
1 — mixture of purified fibrin desAB, D-dimer and D-fragment that was applied to the column and was used as a marker; *2* — fraction eluted at the volume 5.5 ml; *3* — fraction eluted at the volume 8 ml; *4* — fraction eluted at the volume 9.5 ml

In particular, the appearance of D- and DD-fragments in the elution zone of 5.5 ml, which does not overlap with the elution zone of individual fragments (7.5–9.5 ml), was detected, indicating the formation of a ternary complex. Densitometry of electropherograms using TotalLab TL-100 demonstrated that the average densities of pixels in bands of fibrin desAB, D-dimer and D-fragment were equal. It means that the ternary complex of fibrin desAB with D-dimer and D-fragment was composed in the approximate ratio of fibrin desAB, D-dimer and D-fragment 1:1:1.

Molecular docking in the HDOCK software was used to establish the spatial arrangement of the D-fragment in relation to the fibrin desAB molecule bound to the D-dimer. The theoretical binding pose is shown in Fig. 2.

Discussion. For the first time, we have obtained the molecular complex of fibrin desAB, D-dimer and D-fragment using size-exclusion chromatography.

Since protofibrils are formed due to intermolecular interactions of fibrin molecules: the central E-region of one molecule interacts with the peripheral D-regions of the other two (DD-E triad), the formation of the DD-E triad occurs primarily due to the interaction of the “A:a” polymerization sites. Therefore, the complex formation of fibrin desAB with D-dimer is understandable and occurs via the mentioned sites. However, the involvement of another D-region in the complex is not obvious.

The main question raised is what sites of interaction are obedient for the involvement of the D-dimer and D-fragment in fibrin desAB. There are several scenarios for how this interaction occurs. The first possibility is that fibrin desAB binds to the D-dimer through the interaction of one

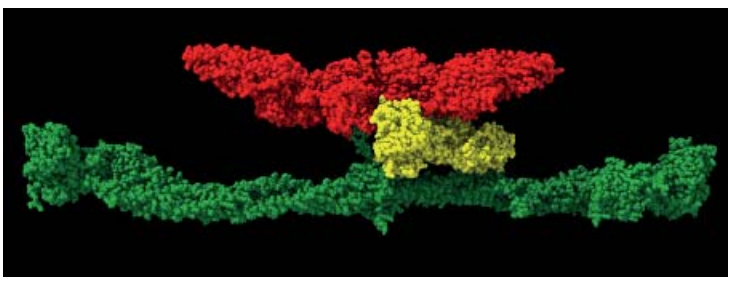

Fig. 2. **Molecular complex of fibrin desAB with D-dimer and D-fragment:**
Green color refers to fibrin molecule, red color — D-dimer and yellow color -— D-fragment

pair of "A:a" sites, while the second pair is involved in the binding of the D-region. Another variant involves the interaction of two pairs of "A:a" sites belonging to fibrin desAB and D-dimer, and the D-fragment is involved through the interaction of the "B:b" site. However, the fact that only one D-fragment is involved remains unclear in this case, since there are two pairs of "B:b" sites. It is possible that the attachment of the second D-fragment is impossible due to conformational clashes caused by conformational changes in the ternary complex.

Conclusions. We obtained and characterized the ternary complex of fibrin desAB, D-dimer and D-fragment by size-exclusion chromatography followed by SDS-PAGE. Further study of the structure and properties of this complex may clarify certain issues related to fibrin polymerization, namely the process of protofibril formation and their spatial branching.

Keywords: fibrin; D-dimer; D-region; fibrin polymerization; docking.

Authors' contribution. OH worked on molecular modeling and size-exclusion chromatography, MS worked on size-exclusion chromatography and SDS-PAGE.

Funding source. The research was financed by the project 0119U002512: "The interaction of the hemostasis system components at the cellular and molecular level in the process of formation and elimination of a thrombus."

Acknowledgement. Authors gratefully acknowledge Prof. Platonova for her help with experiments.

REFERENCES

1. *Weisel J. W., Litvinov R. I.* Mechanisms of fibrin polymerization and clinical implications. *Blood*. 2013; 121(10): 1712–1719. https://doi.org/10.1182/blood-2012-09-306639
2. *Riedel T., Suttnar J., Brynda E., Houska M., Medved L., Dyr J.E.* Fibrinopeptides A and B release in the process of surface fibrin formation. *Blood*. 2011, 3;117(5):1700-6. https://doi.org/10.1182/blood-2010-08-300301.
3. *Lord S. T.* Molecular mechanisms affecting fibrin structure and stability. *Arterioscler Thromb Vasc Biol*. 2011, 31(3): 494–499. https://doi.org/10.1161/ATVBAHA.110.213389.
4. *Gorkun O. V., Veklich Y. I., Medved L. V., Henschen A. H., Weisel J. W.* Role of the alpha C domains of fibrin in clot formation. *Biochemistry*. 1994, 7;33(22): 6986–97. https://doi.org/10.1021/bi00188a031.
5. *Varetska T.* Microheterogeneity of fibrinogen. Cryofibrinogen Ukr. Biochem. J. 1960, 32: 13–24.
6. *Wu H.C., Yen C.C., Tsui W.H., Chen H.M.* A red line not to cross: evaluating the limitation and properness of gel image tuning procedures. *Anal Biochem.* 2010, 1;396(1): 42–50. https://doi.org/10.1016/j.ab.2009.08.041.
7. *Zhmurov A., Protopopova A. D., Litvinov R. I., Zhukov P., Weisel J. W., Barsegov V.* Atomic Structural Models of Fibrin Oligomers. *Structure*. 2018, 5;26(6): 857–868.e4. https://doi.org/10.1016/j.str.2018.04.005.
8. *Yan Y., Zhang D., Zhou P., Li B., Huang S. Y.* HDOCK: a web server for protein-protein and protein-DNA/RNA docking based on a hybrid strategy. *Nucleic Acids Res*. 2017, 3;45(W1): W365–W373. https://doi.org/10.1093/nar/gkx407.
9. *Mayer C. L., Snyder W. K., Swietlicka M. A., Vanschoiack A. D., Austin C. R., McFarland B. J.* Size-exclusion chromatography can identify faster-associating protein complexes and evaluate design strategies. *BMC Res Notes*. 2009, 15;2: 135. https://doi.org/10.1186/1756-0500-2-135.

UDC 577.2 https://doi.org/10.15407/biotech16.02.024

ACTION OF VENOM OF *Vipera lebetina* ON BLOOD COAGULATION *in vitro*

E. ISKANDAROV [1, 2], *A. DMYTRUK* [1,3]

[1]Palladin Institute of biochemistry of the National Academy of Sciences of Ukraine
[2]Biology And Medicine Institute Science Educational Center
of Taras Shevchenko National University Of Kyiv, Ukraine
[3]National Technical University of Ukraine "Igor Sikorsky Kyiv Polytechnic Institute", Ukraine

E-mail: iskandarov.e.sh@gmail.com

Received 2023/04/03
Revised 2023/04/11
Accepted 2023/04/28

Hemorrhagic action caused by phospholipases is the main toxic action of *Vipera* snakes' venom [1]. However, action on the proteins of blood coagulation system is also spread widely among these toxins. Proteases with unique specificity are known tools for the studying structure and functions of blood coagulation system proteins. Even venoms with prevalence of hemolytic or neurotoxic action can contain a wide range of proteases that are of interest for biotechnology and drug development.

Aim. In this study we focused on the search of fibrinogen-targeted proteases in the venom of *Vipera lebetina*.

Methods. Fractionation of the venom was performed using FPLC chromatographic system Acta Prime on Q Sepharose. Analysis of protein mixtures was performed using SDS-PAGE. Action on blood coagulation system was analyzed using APTT assay [2]. Proteolytic action on fibrinogen and identification of protein components with fibrinolytic activity was performed using electrophoresis of mixture of fibrinogen solution (2 mg/ml) with venom`s fractions. For a comprehensive evaluation of the effect of the obtained fractions on hemostasis, an original approach with modified aggregatometry was used [3]. This approach made it possible to take into account the ability of fractions to activate platelets, initiate blood coagulation, or inhibit platelet aggregation. Hemolytic action of fractions was estimated using fresh human red cells. Amount of released hemoglobin was estimated by spectrophotometry on Optizen POP.

Results. Crude venom of *V. lebetina* was fractionated using ion-exchange chromatography on Q Sepharose. Elution was performed using a stepwise gradient of NaCl (0.1, 0.2, 0.3, 0.5, and 0.7 M NaCl) in 0.05 M Tris-HCl buffer at pH 8.3. Fractions eluted at 0.1 and 0.2 M of NaCl contained several proteins with different molecular weights ranging from 75 kDa to low molecular weight fractions according to the SDS-PAGE. In particular, it was necessary to isolate the major fraction with a molecular weight of approximately 20 kDa in fraction 0.1. In fractions 0.3, 0.5, and 0.7, proteins were present in small concentrations. Proteins that cleave α- and β-chains of fibrinogen were found in fractions 0.1 and 0.2, indicating the presence of an enzyme with fibrinogenolytic activity in the venom of *V. lebetina*. The fractions 0.3, 0.5, and 0.7 did not show any significant fibrinogenolytic activity. After platelet aggregation study we concluded that fraction 0.1 contained a protein with fibrinogenolytic activity. An increase in platelet aggregation was observed for the fraction 0.2 after the addition of ADP. This may indicate the presence of an active compound that promotes platelet aggregation. Further research is necessary to determine its nature. Fractions 0.3, 0.5, and 0.7 had no effect on platelet aggregation. A decrease in blood plasma clotting time in APTT to 5 s and 7 s, compared to a control value of 70 s, was shown for fractions eluted at NaCl concentrations of 0.1 M and 0.2 M, respectively. The fractions 0.3, 0.5 had only a slight effect on reducing blood plasma clotting. A slightly increased level of hemolysis was shown in the presence of the unbound fraction and the whole venom. It can be suggested that proteins with phospholipase activity are present in the non-binded fraction.

Table 1

Results of the complex analysis of *Vipera lebetina* snake venom fractions

	Reduction of the clotting time of plasma	Hemolysis of red cells	Fibrinogen cleavage	Inhibition of platelet aggregation
N.B.*	+	+	+	+
0.1	+	–	+	+
0.2	+	–	+	–
0.3	+	–	–	–
0.5	+	–	–	–
0.7	–	–	–	–

* — NB is the fraction that did not bind to the Q sepharose under present conditions. 0.1, 0.2, 0.3, 0.5, 0.7 — fractions eluted at a NaCl concentration of 0.1, 0.2, 0.3, 0.5, and 0.7 M NaCl M respectively).

Discussion. Thus, during the study we demonstrated the presence of proteins in *V. lebetina* venom with fibrinogenolytic activity and proteins that initiate the plasma coagulation time in the APTT test and may have properties of a thrombin-like enzyme or prothrombin activator. Based on our findings, *V. lebetina* venom can be used as a source for obtaining proteins with thrombin-like or prothrombin activating effects (Table 1). Also, we have to keep in mind that several purified snake venom proteins have become significant devices in fundamental exploration and in diagnostic procedures in hemostasis study. That is why further studies of fibrinogen-specific proteases of these species' venoms are promising.

Conclusions. Thus, fibrinogen-specific proteases, hemolytic agents, activators of blood clotting were found in the venom of *Vipera lebetina*. Most of these compounds must to be purified and can be used for basic biochemical research.

Keywords: snake venom; *Vipera lebetina*; fibrinogenolytic action; protease, APTT; aggregatometry; hemostasis.

Acknowledgement. Authors gratefully acknowledged Dr Chernyshenko for his encouragement of these studies.

Authors' contribution. EI fractionated venom of *V. lebetina* and performed measurements, AD performed data analysis and help in the study.

Funding source. The research was financed by the project 0119U002512: "The interaction of the hemostasis system components at the cellular and molecular level in the process of formation and elimination of a thrombus."

REFERENCES

1. *Fernandes C.A., Borges R.J., Lomonte B., Fontes M.R.* A structure-based proposal for a comprehensive myotoxic mechanism of phospholipase A2-like proteins from viperid snake venoms. *Biochim Biophys Acta*. 2014, 1844(12), 2265–2276. https://doi.org/10.1016/j.bbapap.2014.09.015 Epub 2014 Sep 30. PMID: 25278377.
2. *Iskandarov E., Zinenko O., Tupikov A., Pitishkina A., Platonov O., Gryshchuk V., Kucheriavyi Y., Stohnii Y.* Action of venom of Vipera snake of Ukraine on blood coagulation *in vitro*. *Biotechnologia Acta*. 2022, 15(2), 56–57. https://doi.org/10.15407/biotech6.02.097
3. *Iskandarov E., Gryshchuk V., Platonov O., Kucheriavyi Y., Slominskyi O., Stohnii Y., Vartanov V., Chernyshenko V.* Fractionation of Vipera berus berus snake venom and detection of bioactive compounds targeted to blood coagulation system, *Southeastern European Medical Journal*. 2022, v. 6, p. 20–31. https://doi.org/10.26332/seemedj.v6i2.256

UDC 613.25:635.356]001.891.53=111(043.2)

https://doi.org/10.15407/biotech16.02.026

CONSUMPTION OF BROCCOLI SPROUTS INCREASED THE ACTIVITY OF GLUTATHIONE-DEPENDENT ANTIOXIDANT ENZYMES IN MURINE LIVER

M. V. IVANOCHKO, O. I. DEMIANCHUK, M. M. BAYLIAK, V. I. LUSHCHAK

Vasyl Stefanyk Precarpathian National University,
Ivano-Frankivsk, Ukraine

E-mail: marian.ivanochko.20@pnu.edu.ua

Received 2023/04/13
Revised 2023/04/21
Accepted 2023/04/28

Consumption of hypercaloric food leads to increased production of reactive oxygen species (ROS) with the development of oxidative stress resulted in obesity and various metabolic disorders.

Broccoli sprouts may have a potential protective effect against obesity and its comorbidities because of high content of bioactive compounds, such as phenolic compounds and isotiocyanate sulforaphane. Sulforaphane is intensively produced in 3–5 day-old broccoli sprouts. This compound was found to be an activator of the Nuclear factor, erythroid 2 like 2 (Nrf2). Nrf2 is transcription factor that inhibits proinflammatory processes and stimulates antioxidant defense mechanisms. Nrf2 targets are glutathione-dependent genes of glutathione-S-transferase (GST) and glutathione peroxidase (GPx). These enzymes use glutathione to neutralize ROS. They form second line of antioxidant defense against oxidative stress while superoxide dismutase (SOD) and catalase are primaly antioxidant enzymes.

The purpose of this work was to investigate effects of the consumption of broccoli sprouts on the activity of antioxidant defense enzymes in the liver of mice fed with a cafeteria diet.

Methods. Eight-month-old C57BL/6J males were divided into 4 groups. First group (Control) consumed basal feed. Second group (Broccoli) consumed basal feed with 5% (w/w) 3-day-old broccoli sprouts (*Brassica oleracea var. Italica*, sort Calabrese). Third group (Cafeteria Diet) consumed a cafeteria diet which consisted of 70% (by mass) products of human ration (peanuts in chocolate, milk chocolate, chocolate cracker) and 30% of basal feed. Fourth group (Cafeteria Diet + Broccoli) consumed combination of a cafeteria diet and broccoli (5% of total food). After 16 weeks mice were euthanized according to bioethics norms with CO_2 anesthesia, murine liver was dissected and frozen in liquid nitrogen.

Frozen tissue was homozeniged in lysis buffer, centrifuged and resulted supernatants were used for analysis. Activities of enzymes were determined by using electrophoresis in polyacrylamide gel by the method of Ramesh et al. [1]. After electrophoresis we conducted dyeing of separate gels for detection of superoxide dismutase (SOD), glutathione-S-transferase (GST) or glutathione peroxidase (GPx) isoforms. Identification of SOD isoforms was carried out by the method of Beauchamp and Fridovich [2]. GST isoforms were detected by the method of Ricci et al. [3]. GPx isoforms were identified by the method of Lin et al. [4]. After photo fixation of gels, we determined activity of each isoform densitometrically using ImageJ software. Results were statistically analyzed by ANOVA followed by post-hoc Tukey's test. Data are presented as mean±SEM.

Results. In the hepatic tissue of all four groups of mice, two isoforms of SOD (SOD1 and SOD2) were detected in gels. The intensity of the bands of both isoforms was not significantly different between groups (Fig. 1). Three isoforms of GST (GST1, GST2, GST3) were detected in the liver samples. The activity of GST1 did not significantly differ between the experimental groups (Fig. 2).

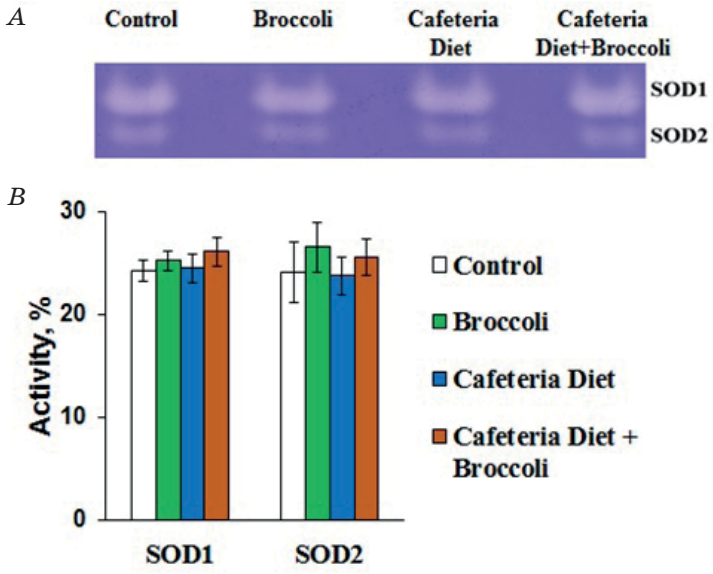

Fig. 1. **Electrophoretic dyed gel pattern (*A*) and the in-gel activity (*B*) of SOD isoforms in the murine liver $n = 5$**

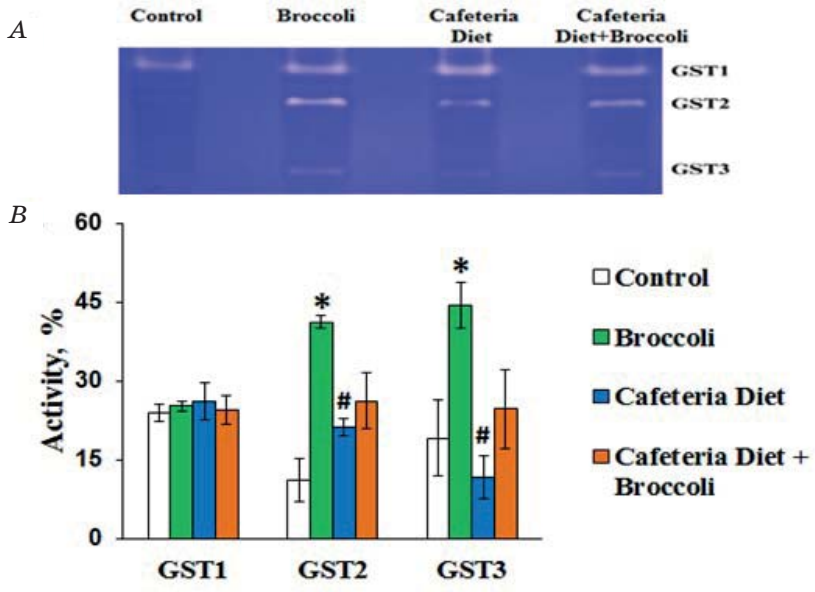

Fig. 2. **Electrophoretic dyed gel pattern (*A*) and the in-gel activity (*B*) of isoforms of glutathione-S-transferase (GST) in murine liver, $n = 3$:**
* — significantly different from the control group, # — significantly different from the Broccoli group

Activities of GST2 and GST3 forms were significantly higher in the group "Broccoli" compared to Control and Cafeteria Diet groups (Fig. 2).

We identified three isoforms of glutathione peroxidase (GPx1, GPx2, GPx3) in liver samples. The activity of GPx isoform 1 was not significantly different between the experimental groups (Fig. 3). The activity of GPx2 was significantly higher in the group of mice that consumed Broccoli and Cafeteria Diet + Broccoli compared to Control. GPx2 activity was significantly higher in the Broccoli group compared to the Cafeteria Diet group. Activity of GPx3 was significantly higher in the Broccoli group compared to the Control and Cafeteria Diet group (Fig. 3).

Discussion. We expected that both cafeteria diet and brocolli spouts would modulate antioxidant enzyme activities in mouse liver, as it was observed in rats fed high-calorie diet with antioxidant plants [1].

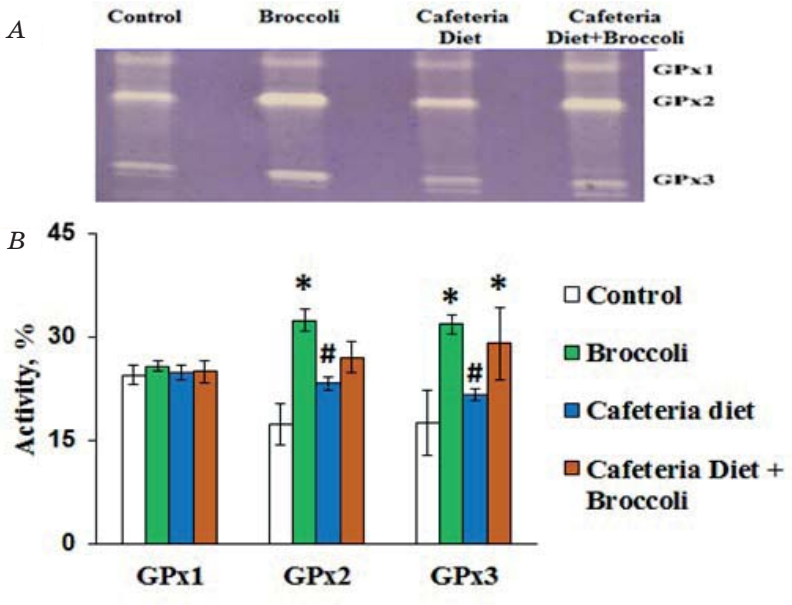

Fig. 3. **Electrophoretic dyed gel pattern (*A*) and the in-gel activity (*B*) of isoforms of glutathione peroxidase (GPx) in murine liver, $n = 4$:**
* — significantly different from the control group according, # — significantly different from the Broccoli group

In our study, enzymes activities were not significant different between control mice and mice fed with cafeteria diet. However, we found an improvement in the functioning of GST2 and GST3 in Broccoli group compared to Control and Cafeteria Diet groups. We may explaine this fact as a result of Nrf2 activation by sulforaphane from broccoli and stimulation of GST2 and GST3 synthesis to neutralize ROS. GPx2 and GPx3 activities were significantly higher in Broccoli group, similarly to GST2 and GST3. The activity of GPx2 in Cafeteria diet + Broccoli group was significantly higher in compare to Control group.

We proposed that during healthy condition and obesity bioactive compound of broccoli sulforaphane had activated Nrf2. Nrf2 in priority increased expression of *GST* and *GPx* genes as his targets for antioxidant defense and left *SOD* without expression. This hypothesis would be tested and supplemented by determination of other antioxidant enzymes and Nrf2 targets.

Conclusions. Cafeteria diet did not significantly affect the activity of SOD isoforms, but led to redistribution of in the activity of GST and GPx isoforms in murine liver. Feeding with broccoli spouts significantly increased the activity of 2 and 3 isoforms of GST and GPx in murine liver compared to values in control mice and mice fed with cafeteria diet. Combination of Broccoli + Cafereria diet had small activating effects on antioxidant enzyme acivity, compared with cafeteria diet.

Key words: obesity; cafeteria diet; Nrf2; broccoli; antioxidant enzymes.

Authors' Contribution. M.V. Ivanochko – performance of experiments (maintenance and feeding of mice, electrophoresis), data analysis, visualization and wtitting of original graft; O.I. Demyanchuk — performance of experiments (electrophoresis); M.M. Bayliak — experimental design, writing — review and editing. V.I. Lushchack — conceptualization, writing — review and editing, funding acquisition.

Funding source. This research was carried out with the support of the Ministry of Education and Science of Ukraine (#0122U000894).

REFERENCES

1. *Ramesh E., Jayakumar T., Elanchezhian R., Sakthivel M., Geraldine P., Thomas P.A.* Green tea catechins, alleviate hepatic lipidemic-oxidative injury in Wistar rats fed an atherogenic diet. *Chem. Biol. Interact*. 2009, 180(1):10–9. https://doi:10.1016/j.cbi.2009.02.013
2. *Beauchamp C., Fridovich I*. Superoxide dismutase: improved assays and an assay applicable to acrylamide gels. *Anal. Biochem*. 1971, 44: 276–287. https://doi.org/10.1016/0003-2697(71)90370-8
3. *Ricci G., Lo Bello M., Caccuri A.M., Galiazzo F., Federici G.* Detection of Glutathione-S-transferase activity on polyacrylamide gels. *Anal. Biochem*. 1984, 143:226–230. https://doi.org/10.1016/0003-2697(84)90657-2
4. *Lin C.L., Chen H.J., Hou W.C.* Activity staining of glutathione peroxidase after electrophoresis on native and sodium dodecylsulfate polyacrylamide gels. *Electrophoresis*. 2002, 23:513–516. https://doi.org/10.1002/1522-2683(200202)23:4%3C513::aid-elps513%3E3.0.co;2-j

UDC 577.2 https://doi.org/10.15407/biotech16.02.030

TRANSMISSION ELECTRON MICROSCOPY FOR THE DIRECT ANALYSIS OF FIBRIN CLOT STRUCTURE

Y. P. KUCHERIAVYI, I. D. PANAS

Palladin Institute of biochemistry of the National Academy of Sciences of Ukraine, Kyiv

E-mail: biophysicist958@gmail.com

Received 2023/03/27
Revised 2023/04/21
Accepted 2023/04/28

Fibrin polymerization is a crucial process of blood clotting that provides the three-dimension core for the blood thrombus. The main approach of studying fibrin polymerization is still turbidimetry based on light absorption of fibrin solution. It allows to estimate both stages of fibrinogen-fibrin conversion. The initial one, which proceeds without any change of turbidity, reflects the process of protofibril formation, and the second stage of lateral aggregation, is characterized by the rise of turbidity [1]. This method is simple and useful. It allows to estimate the effects of exogenous factors of fibrin polymerization as well as the changes and blood plasma ability to coagulate in pathological conditions.

However, this method has several limitations. First of all, the lag-period of turbidity curve can indicate both inhibition of protofibrils formation and their self-assembly. Also, the final turbidity of the clot is strongly dependent not only on the effectiveness of clotting, but also on the structure of the clot that was obtained. Thick fibrils can be more transparent than the network of thin pathological fibrils. Only confident way to analyze the structure and the mechanisms of formation of fibrin clot is the transmission electron microscopy (TEM) [2].

Aim. The purpose of our study was to compare the structure of clots formed as a result of thrombin-induced fibrin polymerization in the presence or absence of monoclonal fibrin-specific antibodies fragments as factors that change the clot structure. We concentrated on the final stage of fibrin clot formation at maximal turbidity point for every sample.

Methods. Fibrin polymerization was studied by transmission electron microscopy (TEM) of negatively contrasted samples on H-600 Transmission Electron Microscope ("Hitachi",Japan); 1% water solution of uranyl acetate ("Merck", Germany) was used as a negative contrast. For sample preparation, in sterile glass tubes were sequentially added 0.32 mg/mL human fibrinogen, 0.025 M $CaCl_2$ in 0.05 M ammonium formiate buffer (pH 7.9), and a total sample volume was 0.22 mL. The polymerization of fibrin was initiated by the introduction of thrombin at a final concentration of 0.25 NIH/mL. After 180 s, aliquots were taken from the polymerization medium. Each aliquot was diluted to a final fibrinogen concentration of 0.07 mg/mL; 0.01 mL probes of fibrinogen solution were transferred to a carbon lattice, which was treated with a 1% uranyl acetate solution after 2 min. Investigations were per-formed using an H-600 electron microscope at 75 kV. Electron microscopic images were obtained at magnification of 20,000–50,000 [3].

Results. Two monoclonal antibodies fragments were obtained towards the mixture of separated Aα-, Bβ- and γ-chains of fibrinogen. Antibodies fragments that were marked as III-1D and I-4A, had different epitopes within fragment Aα 105–206 of D-region of fibrinogen.

It was shown that addition of antibody fragment I-4A lead to formation of abnormal fibrils that were thinner than in the control sample and were organized in the dense network (Figure). Control sample exhibited the thick fibrils with well-structured classically organized network. The difference between control and I-4A samples demonstrated that antibody I-4A disrupted the structure of polymerized fibrin. In the same time the fibrils obtained in the presence of antibody fragment III-1D were closer to the control ones (Figure).

Discussion. TEM allowed to demonstrate the difference in the action of antibody fragments III-1D and I-4A on thrombin-induced fibrin polymerization. Despite that fact that these antibodies fragments were targeted to the same zone Aα 105–206, they acted on the process in a different

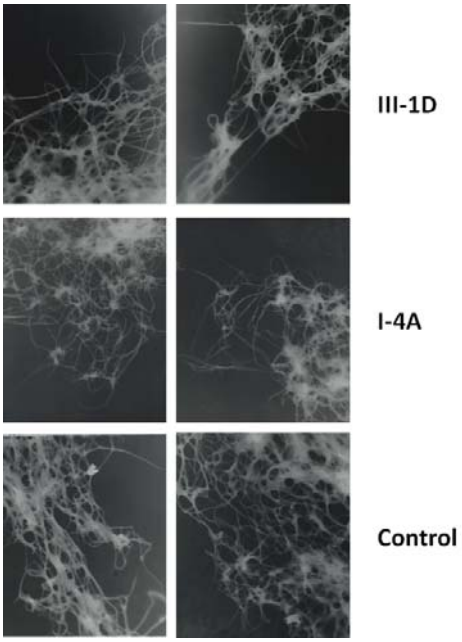

Figure. **Electron microscopy of polymerized fibrin at a point of maximal turbidity:**
III-1D — in the presence of monoclonal anti-Aα105-206 antibody fragment III-1D;
I-4A — in the presence of monoclonal anti-Aα105-206 antibody fragment I-4A;
control — without addition of monoclonal antibodies fragments

manner. This fact allowed us to assume the different functional properties of sites that correspond to the epitope of the studied antibodies fragments.

Conclusions. TEM is an informative method for the study of the fibrin network formation. Its application allows to estimate the disruption in fi brin formation directly. In a combination with turbidity study and other functional tests TEM can provide important information about molecular mechanisms of clot formation.

Key words: fibrin; TEM; fab; polymerization; fibrils; antibody fragment.

Acknowledgement. Authors gratefully acknowledge Prof. Platonova for her help with experiments.

Authors' contribution. Authors contributed to the work equally.

Funding source. Research was supported by the ALLEA grant EFDS-FL2-02 provided to the Institution within the framework of Funding Line 2 of the"European Fund for Displaced Scientists" (EFDS).

REFERENCES

1. *Weisel J. W., Nagaswami C.* Computer modeling of fibrin polymerization kinetics correlated with electron microscope and turbidity observations: clot structure and assembly are kinetically controlled. *Biophys J.* 1992 Jul;63(1), 111–128. https://doi.org/10.1016/S0006-3495(92)81594-1 PMID: 1420861; PMCID: PMC1262129.
2. *Chernysh I. N., Nagaswami C., Weisel J. W.* Visualization and identification of the structures formed during early stages of fibrin polymerization. *Blood*. 2011 Apr 28;117(17), 4609–4614. https://doi.org/10.1182/blood-2010-07-297671 Epub 2011 Jan 19. PMID: 21248064; PMCID: PMC3099577.
3. *Stohnii Y. M., Sakovich V. V., Chernyshenko V. O., Chernishov V. I., Chernyshenko T. M., Kolesnikova I., Kucheriavyi Y. P., Zhernossekov D. D.* Fibrinogenolytic activity of protease from the culture fluid of Pleurotus ostreatus. *Journal of Biological Research — Bollettino Della Società Italiana Di Biologia Sperimentale*, 2020, 93(2). https://doi.org/10.4081/jbr.2020.9006

UDC 57.577 https://doi.org/10.15407/biotech16.02.032

STRUCTURAL PATTERNS OF IVERMECTIN ALLOSTERIC INTERACTION WITH GLUTAMATE-GATED CHLORIDE CHANNEL OF *Caenorhabditis elegans*

Y. O. KUSTOVSKIY[1,2], *A. I. YEMETS*[1,2]

[1]Institute of Food Biotechnology and Genomics
of the National Academy of Sciences of Ukraine, Kyiv
[2]National University of Kyiv Mohyla Academy, Ukraine

E-mail: ykustovskiy@gmail.com

Received 2023/03/30
Revised 2023/04/04
Accepted 2023/04/28

The drug repurposing, which is the search of new applications for known bioactive compounds, has apparent benefits (e.g., cost efficiency, development risks, and time reduction) as compared to the traditional *de novo* drug design making it common for different research fields including the biological drug discovery [1]. The nematocide and insecticide ivermectin (IVM) is considered a wide spectrum agent, which makes it a perspective candidade for repurposing [2]. Although the structure-activity relationships of IVM interactions with its traditional targets of Cys-loop receptors family are studied [3], their structural patterns have not been described yet. The knowledge of structural patterns, which are groups of residues related spatially and by physico-chemical properties, with high affinity for IVM functional groups can be used to find local similarities in active sites of IVM potential targets when the direct alignment of sites cannot be implemented due to the evolutionary distinction between known and potential targets [4].

Aim. To determine the structural patterns of IVM allosteric interaction with residues of its binding site located in the transmembrane domain of α-homopentameric glutamate-gated chloride channel (GluClα) of *Caenorhabditis elegans*.

Methods. To consider different conformational states of IVM binding site two complexes of IVM bound to *C. elegans* GluClα (each with five site conformations) with identifiers 3RHW (https://doi.org/10.2210/pdb3RHW/pdb) and 3RIF (https://doi.org/10.2210/pdb3RIF/pdb) were obtained from PDB [5]. The structures were examined in Analyzer Mode of SeeSAR v.12.1.0, in which contributions of IVM atoms into the complex affinity and their interactions with site structural patterns were determined for each site conformation using the HYDE scoring function [6]. The residues belonging to identified structural patterns were classified by their properties using the Taylor's classification of amino acids [7].

Results and Discussions. The binding site of IVM on cys-loop receptors including GluClα is located in the interface between transmembrane domains of (+) and (−) subunits and is formed by M2, M3, and M2-M3 of (+) subunit and M1 of (−) subunit (Fig. 1, *A*). As it is demonstrated on the Fig. 1, *B*, IVM is composed of the 16-membered heteromacrocyclic ring fused with the spiroketal and benzofuran groups, and linked with the disaccharide group.

According to the results, the benzofuran group is critical for IVM recognition and binding: it interacts with the T-A-S-N-D-I-L-Q-I-P pattern, which is formed by T257, A258, S260, and N264 of M2, D277 and I280 of M3 of (+) subunit and L218, Q219, I222, P223 of M1 of (−) subunit (Fig. 2, *A*). Due to the size and hydrophobicity of macrocycle, its different parts interact with residues of all site-forming structural elements mentioned above resulting in the V-I-G-A-M and I-V-D-L patterns demonstrated on the Fig. 2, *B, C*. While the V-I-G-A-M pattern is formed by the residues of (+) subunit (V278, I280, G281, A282, and M284 of M3), the I-V-D-L pattern contains residues of both subunits: I273 of M2-M3, D277 and V278 of M3 of (+) subunit and L218 of M1 of (−) subunit. Finally, the spiroketal group interacts with M-T-F-C-M-I of (+) subunit (M284, T285, and F288 of

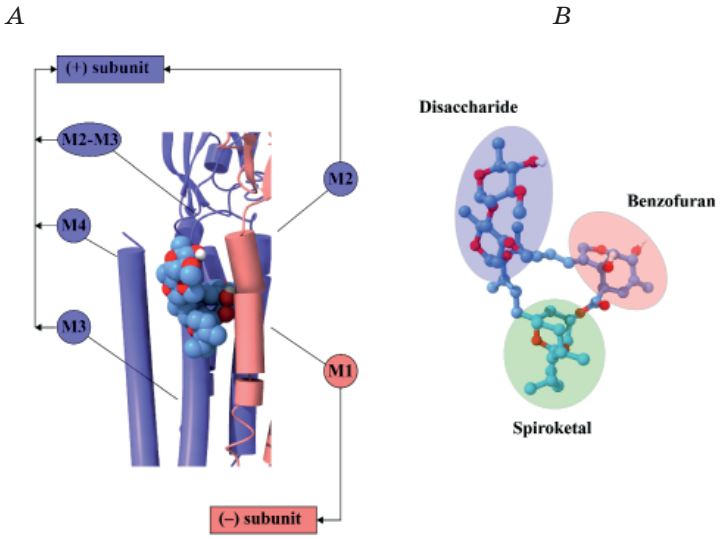

Fig. 1. **The binding site of IVM on GluClα (*A*) and the bioactive conformation of IVM (*B*) visualized using the UCSF ChimeraX v. 1.5 [8]**

M3) and (–) subunit (C225, M226, and I229 of M1) (Fig. 2, *C*). As opposed to other functional groups, the disaccharide is located outside of the binding site pocket. It interacts with I273 of M2-M3 of (+) subunit and L217, L218, and I222 of M1 of (–) subunit; however, considering that these residues are not united spatially, no pattern for the disaccharide can be determined based on the structural information which was analyzed. The determined structural patterns of IVM allosteric interaction with GluClα can be used in search of IVM binding site on its potential targets, in the development of hypotheses of IVM binding to identified sites, and to rationalize the drug design of new GluCl ligands.

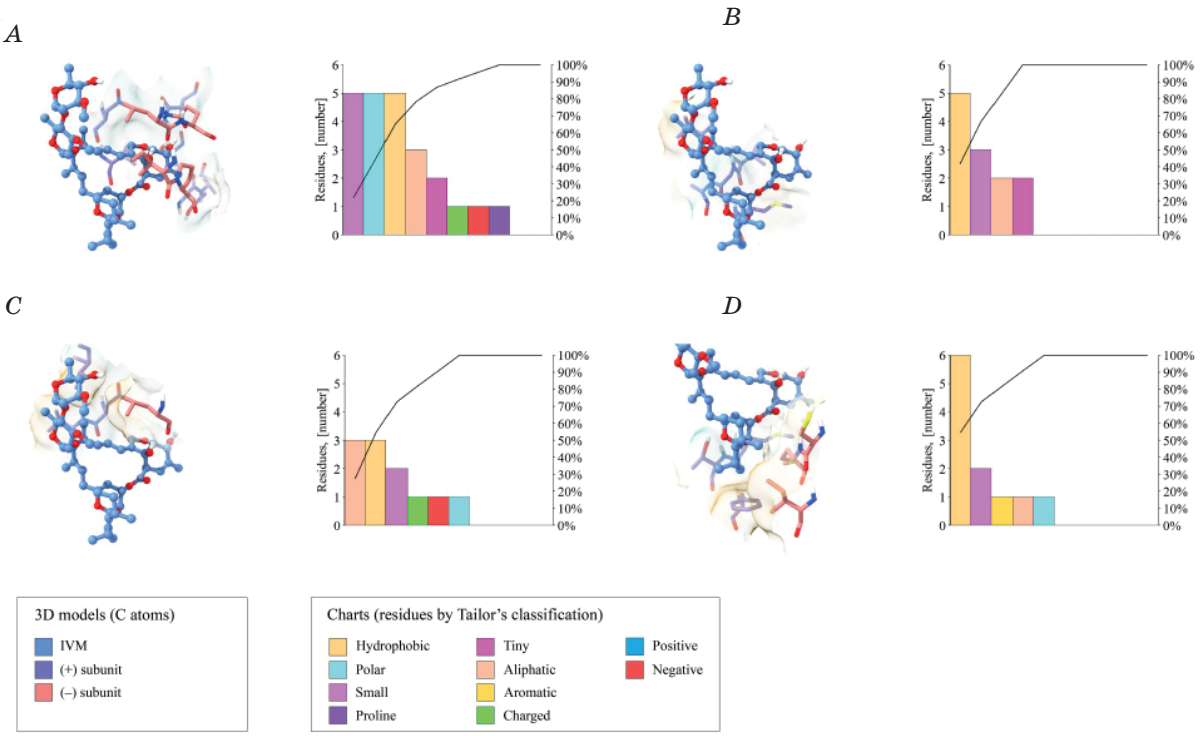

Fig. 2. **The identified structural patterns with high affinity for IVM functional groups:**
A — T-A-S-N-D-I-L-Q-I-P; *B* — V-I-G-A-M; *C* — I-V-D-L; *D* — M-T-F-C-M-I:
the physico-chemical properties of their residues, which were determined based on the Taylor's classification of amino acids, are represented on the respective graphs

Conclusions. The structural patterns with high affinity for IVM functional groups have been determined based on the results of HYDE assessment and visual analysis of IVM-GluClα complexes and the possible implementations of patterns knowledge have been described. The identified patterns can be further corrected and extended using the structural information of other IVM targets deposited in PDB.

Key words: ivermectin; drug repurposing; *Caenorhabditis elegans*; glutamate-gated chloride channels; *in silico* molecular modeling.

Authors' contribution. The YOK performed analysis of structural information and wrote the first draft. AIY formulated the concept of research and supervised the project. Both authors contributed equally to final writing.

Funding source. The work was funded by the National Academy of Sciences of Ukraine (КПКВК 6541230).

REFERENCES

1. *Mittal N., Mittal R.* Repurposing old molecules for new indications: defining pillars of success from lessons in the past. *Eur. J. Pharmacol*. 2021, 912 (4), 1–12. https://doi.org/10.1016/j.ejphar.2021.174569
2. *Martin R. J., Robertson A. P., Choudhary S*. Ivermectin: an anthelmintic, an insecticide, and much more. *Trends Parasitol*. 2021, 37 (1), 48–64. https://doi.org/10.1016/j.pt.2020.10.005
3. *Chen I. S., Kubo Y*. Ivermectin and its target molecules: shared and unique modulation mechanisms of ion channels and receptors by ivermectin. *J. Physiol*. 2018, 596 (10), 1833–1845. https://doi.org/10.1113/jp275236
4. *Salentin S., Haupt V. J., Daminelli S., Schroeder M*. Polypharmacology rescored: protein–ligand interaction profiles for remote binding site similarity assessment. *Prog. Biophys. Mol. Biol*. 2014, 116 (2–3), 174–186. https://doi.org/10.1016/j.pbiomolbio.2014.05.006
5. *Hibbs R. E., Gouaux E*. Principles of activation and permeation in an anion-selective Cys-loop receptor. *Nature*. 2011, 474 (7349), 54–60. https://doi.org/10.1038/nature10139
6. *Schneider N., Lange G., Hindle S., Klein R., Rarey M*. A consistent description of HYdrogen bond and DEhydration energies in protein–ligand complexes: methods behind the HYDE scoring function. *J. Comput. Aided Mol. Des*. 2013, 27 (1), 15–29. https://doi.org/10.1007/s10822-012-9626-2
7. *Valdar W. S. J*. Scoring residue conservation. *Proteins*. 2001, 48 (2), 227–241. https://doi.org/10.1002/prot.10146
8. *Pettersen E. F., Goddard T. D., Huang C. C., Meng E. C., Couch G. S., Croll T. I., Morris J. H., Ferrin T. E*. UCSF ChimeraX: Structure visualization for researchers, educators, and developers. *Protein Sci*. 2021, 30 (1), 70–82. https://doi.org/10.1002/pro.3943

UDC 57; 616-092 https://doi.org/10.15407/biotech16.02.035

EFFECTS OF IMIDOPYRAN AND PREDNISONE IN THE TREATMENT OF BABESIOSIOSIS-ASSOCIATED ANEMIA IN DOGS

A.Y. NEVIDNYK-PRAVDA

Oles Honchar Dnipro National University, Ukraine

E-mail: aaasssaaa079@gmail.com

Received 2023/03/23
Revised 2023/04/05
Accepted 2023/04/28

Anemia is one of the most widespread animal diseases. It is not an exception for dogs in which the development of hemolytic anemia occurs against the background of babesiosis [1]. Studying the features of the development and treatment of hemolytic anemia in dogs is an urgent problem in veterinary laboratory practice [2]. At this stage, it is important to understand the specifics of treatment and their impact on improving the animal's condition and recovery.

Aim. To investigate the development and treatment with imidopyran and prednisolone of hemolytic anemia in dogs caused by the protozoan parasite *Babesia canis*.

Methods. 17 domestic dogs weighing 5–10 kg aged 2–5 years were used for the study. The parameters of the general blood analysis were determined using the MicroCC-20 Plus automated hematology analyzer (HTI, USA). Microscopy with a Leica DM4 electric microscope (Germany) was carried out to study the condition of erythrocytes, counting the number of leukocytes and platelets.

Results. The main indicator of the development of anemia in animals is the number of erythrocytes, hemoglobin, and hematocrit. Development of babesiosis lead to the hemolytic anemia investigated in dogs before treatment: the number of erythrocytes lower than normal by 20–30%, the level of hemoglobin 40–55%, the average concentration of hemoglobin in erythrocytes 10–18%, hematocrit 20–30% and the number of platelets 40–50%.

he main period of the treatment of babesiosis in dogs is the first 24 hours with imidopyran (Arterium, Ukraine, dose 7 mg/kg) and prednisone (Darnytsia, Ukraine, dose 2.2 mg/kg) with simultaneous use in the form of injections that improved all parameters of the general blood test. The number of erythrocytes increased from the previous results by 15–20% (Fig. *A*), the level of hemoglobin by 10–15%, the average concentration of hemoglobin in erythrocytes by 5–10%, hematocrit by 22% (Fig. *B*) and the number of platelets by 10–15%.

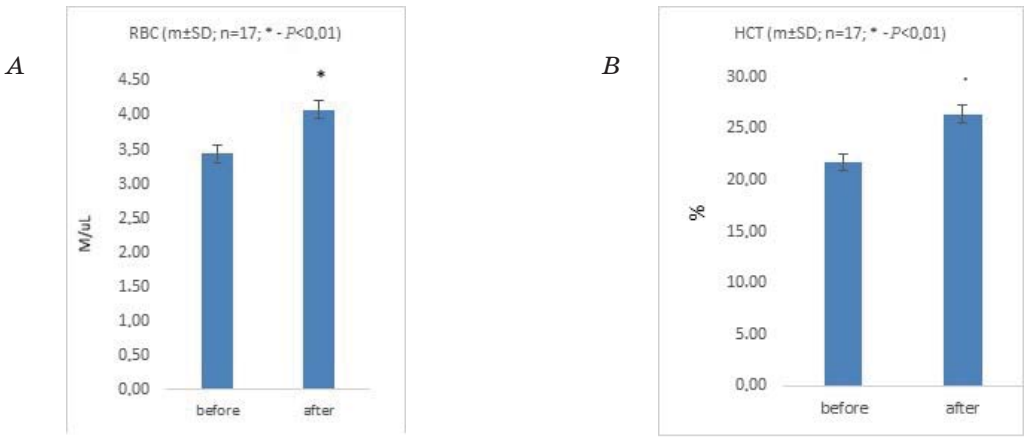

Figure. **Values of erythrocytes (*A*) and hematocrit (*B*) in the dog`s blood before and after treatment with imidopyran and prednisolone**

Conclusions. The results of the study showed that treatment with imidopyran and prednisolone is effective in cases of babesiosis for dogs caused by the protozoan parasite *Babesia canis*. Moreover, such treatment decreases the risks of the anemic state development for these animals.

Keywords: canine anemia; hemorrhagic anemia; imidopyran; prednisone; babesiosis.

Funding. The scientific work was carried out within the framework of the dissertation work at the expense of the basic funding of the Ministry of Education and Science of Ukraine (N BF/6-2021)

REFERENCES

1. *Cuq B., Blois S. L., Mathews K. A.* Anti-thymocyte serum as part of an immunosuppressive regimen in treating haematological immune-mediated diseases in dogs. *J. Small Anim. Pract.* 2017, v. 58, p. 348–354. https://doi.org/10.1111/jsap.12666 Epub 2017 Mar 28.
2. *Lobetti R.* Changes in the serum urea: creatinine ratio in dogs with babesiosis, haemolytic anaemia, and experimental haemoglobinaemia. *Vet. J.* 2012, v. 191, p.:253–256. https://doi.org/10.1016/j.tvjl.2011.01.027 Epub 2011 Mar 12.
3. *Kane B. K., Greer R. M.* Human intravenous immunoglobulin use for hematological immune-mediated disease in dogs. *J. Am. Vet. Med. Assoc.* 2023. https://doi.org/10.2460/javma.23.01.0043 Online ahead of print.13.

UDC 606:61 **https://doi.org/10.15407/biotech16.02.037**

Ex vivo STUDY OF THE ACTION OF INTEGRIN RECEPTORS ANTAGONIST FROM ECHIS MULTISQUAMATIS SNAKE VENOM ON PLATELETS OF PREGNANT WOMEN WITH COMPICATIONS DURING GESTATION

O. M. PLATONOV[1], *I. V. US*[2]

[1]Palladin Institute of Biochemistry
of the National Academy of Sciences of Ukraine, Kyiv
[2]The Shupyk National Medical Academy of Postgraduate Education, Kyiv, Ukraine

E-mail: chaosplaton@gmail.com

Received 2023/03/23
Revised 2023/04/05
Accepted 2023/04/28

Disorders of hemostasis system during gestation period is worldwide problem that influence, more or less, life of approximately 1/8 pregnant women [1]. The application of different methods to study problems that occur during pregnancy will allow defining and solving the risks during this period and give solutions for the preventing of complications. Elevated platelet function is an important part of pathogenesis of placenta dysfunctions and also a risk-factor for thrombotic events during pregnancy.

The issue of resistance to the most important antiplatelet drugs remains quite relevant. Aspirin is the most important antiplatelet agent in obstetrics, which has been proven as a means of preventing vascular-placental complications. At the same time, aspirin, as the gold standard of antiplatelet strategy, does not show the expected antiplatelet effect in 5–40% of patients [2]. Therefore, the search for new effective antiplatelet drugs and controlled antithrombotic prophylaxis to prevent placenta-associated pregnancy complications is an important task.

Aim. In our work, we studied platelet aggregation in blood plasma of pregnant women and estimated the possibility of *ex vivo* normalization of aggregation rate using a polypeptide from the *Echis multisquamatus* snake venom. Previous reports demonstrated that it directly interacts with glycoprotein IIb/IIIa receptors on the surface of platelets, preventing their adhesion, thereby affecting the degree of aggregation [3].

Methods. Crude venom of *Echis multisquamatus* was fractionated using ion-exchange chromatography followed by size-exclusion chromatography on Superdex 75 using the FPLC system (ÄKTA, GE Healthcare, USA). Analysis of molecular weight of protein components was performed using SDS-PAGE. The concentration of protein was measured using spectrophotometer Optizen POP (Korea) at 280 nm. The ability of obtained protein to inhibit platelet aggregation was measured directly by aggregometry. Blood samples of women with placental disfunction during pregnancy (n = 28) were kindly provided by "Perinatal Center of Kyiv". This study was approved by the Ethics Commission of the Shupyk National Medical Academy of Postgraduate Education and the Ethics Commission of the Kyiv Perinatal Center (# 3 from 05/05/2020). Aggregation of platelet-rich plasma (PRP) induced by ADP was investigated using aggregometry on the AP 2110 (Solar, Belarus). We compared the rate of platelet aggregation in the presence vs absence of platelet aggregation inhibitor.

Results. Two-step chromatography protocol allowed us to obtain the polypeptide from the venom of *Echis multisquamatus* that possessed the anti-aggregatory action. SDS-PAGE analysis confirmed the homogeneity of obtained polypeptide with apparent molecular weight 14 kDa that corresponds to the platelet aggregation inhibitor reported earlier [3]. Initial studies of ADP-induced platelet aggregation allowed selecting active concentration for the effective inhibitory action as 0.02 mg/ml.

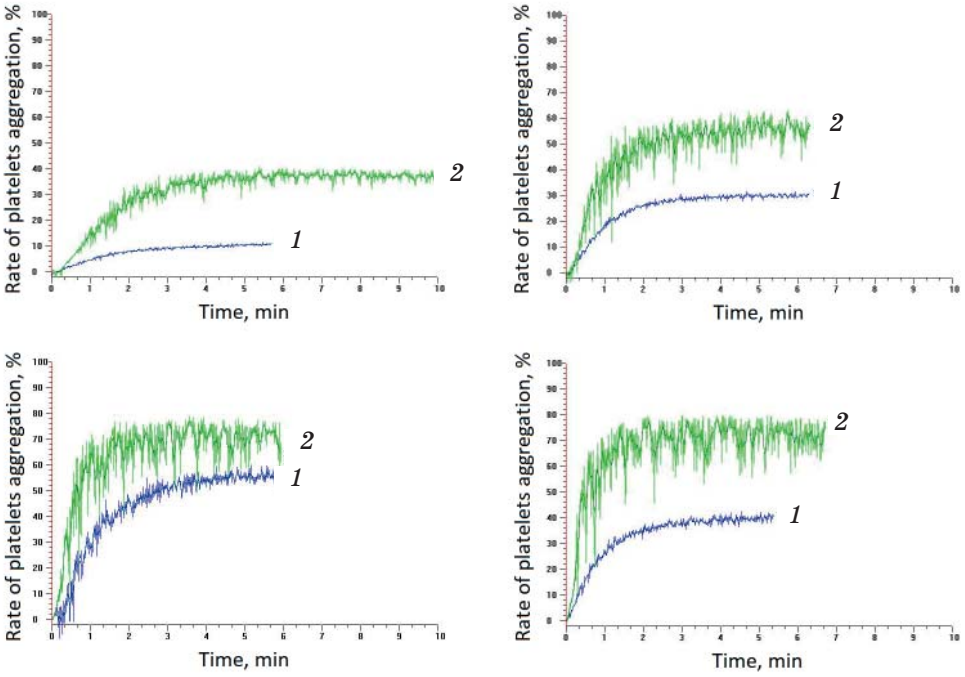

Figure. **ADP-induced aggregation of platelets in the platelet rich blood plasma of pregnant women with complicated pregnancy:**
1 — with adding of integrin receptors antagonist, *2* — control sample

Platelet aggregation in platelet rich plasma of pregnant women was measured immediately after blood collection. Polypeptide was added to the PRP at the final concentration 0.02 mg/ml. Platelets were activated by ADP immediately after that without pre-incubation. Inhibitory effect of studied polypeptide was shown for all analyzed samples of platelet rich blood plasma without the exceptions (Figure). In particular, it inhibited ADP-induced platelet aggregation in the range of 30–60%.

Discussion. Integrin receptors antagonists bind to receptors mainly through tripeptide motifs RGD [4]. Drugs based on RGD-containing snake venom disintegrins effectively inhibit platelet aggregation by blocking binding between neighboring platelets through its main ligand fibrinogen [5]. Effective inhibitory effect on platelets aggregation provides new opportunities for the use of disintegrins to develop the universal anti-aggregatory approaches that can be effective independently of individual peculiarities of patients. Taking into account the fact that integrins function not only as intercellular adhesive receptors, but also as cell-substrate receptors and are of great importance in the migration of leukocytes to the center of inflammation, further studies of anti-integrin agents in patients with vascular-placental complications, when the processes of sterile inflammation in the placenta are activated [6], look quite attractive.

Conclusions. Platelet aggregation inhibitor from *Echis multisquamatis* snake venom of can be assumed as the effective agent that reduce the rate of platelet aggregation. We demonstrated it efficacy in platelet rich plasma of pregnant women that had placenta dysfunction. The use of direct antagonist of platelet integrin receptors was assumed as the prospective approach for suppressing of platelet reactivity in particular during complicated pregnancy.

Key words: snake venom; disintegrin; aggregation of platelets; pregnancy; glycoprotein IIb/IIIa.

Ethical Committee Approval: # 3 from 2020/05/05/.

Author's contribution. O. M. Platonov performed ion-exchange chromatography, SDS-PAGE and aggregometry, I. V. Us supervised and monitored the patients.

Funding source. The research was financed by the project 0119U002512: "The interaction of the hemostasis system components at the cellular and molecular level in the process of formation and elimination of a thrombus.

Acknowledgement. Authors gratefully acknowledge Prof. S.I. Zhuk and Dr. V. O. Chernysheko for their contribution to this work.

REFERENCES

1. *Danilack V. A., Nunes A. P., Phipps M. G.* Unexpected complications of low-risk pregnancies in the United States. *American journal of obstetrics and gynecology*. 2015, 212(6), 809.e1–809.e6. https://doi.org/10.1016/j.ajog.2015.03.038
2. *Bij de Weg, J. M., Abheiden, C. N. H., Fuijkschot, W. W., Harmsze, A. M., de Boer, M. A., Thijs, A., & de Vries, J. I. P.* Resistance of aspirin during and after pregnancy: A longitudinal cohort study. *Pregnancy hypertension*, 2020, v. 19, p. 25–30. https://doi.org/10.1016/j.preghy.2019.11.008
3. *Chernyshenko V., Petruk N., Korolova D., Kasatkina L., Gornytska O., Platonova T., Chernyshenko T., Rebriev A., Dzhus O., Garmanchuk L., Lugovskoy E.* Antiplatelet and anti-proliferative action of disintegrin from Echis multisquamatis snake venom. *Croatian medical journal*. 2017, 58(2), 118–127. https://doi.org/10.3325/cmj.2017.58.118
4. *Vasconcelos A. A., Estrada J. C., David V., Wermelinger L. S., Almeida F. C. L., Zingali R. B.* Structure-Function Relationship of the Disintegrin Family: Sequence Signature and Integrin Interaction. *Frontiers in molecular biosciences*. 2021, v. 8, p. 783301. https://doi.org/10.3389/fmolb.2021.783301
5. *Lazarovici P., Marcinkiewicz C., Lelkes P. I.* From Snake Venom's Disintegrins and C-Type Lectins to Anti-Platelet Drugs. *Toxins*, 2019, 11(5), 303. https://doi.org/10.3390/toxins1105030
6. *Moser G., Guettler J., Forstner D., Gauster M.* Maternal Platelets-Friend or Foe of the Human Placenta?. *International journal of molecular sciences*, 2019, 20(22), 5639. https://doi.org/10.3390/ijms20225639

UDC: 616.314.17:616.89:599.323.4:612.08 https://doi.org/10.15407/biotech16.02.040

ROLE OF NO IN SOFT PERIODONTAL TISSUES OF RATS DURING STRESS AND INFLAMMATION

PLETNOV V. V., TKACHENKO O. T., MYKYTENKO A. O.

Poltava State Medical University, Ukraine

E-mail: pletnew200211@gmail.com

Received 2023/03/14
Revised 2023/04/24
Accepted 2023/04/28

Bacterial lipopolysaccharide (LPS) induces the formation of nitric oxide (NO) and proinflammatory cytokines by activating nuclear factor κB (NF-κB) signaling pathways through toll-like receptor 4 (TLR4), which leads to destruction of periodontal soft tissues, including resorption of alveolar bones [1]. The Scientific School of Professor Tarasenko L.M. substantiated biochemical mechanisms of stress-induced periodontal tissue damage [2]. Chronic stress leads to an imbalance in the immune homeostasis of periodontal tissues, which can lead to the development of chronic periodontitis and/or increase the destruction of biopolymers of periodontal tissues [3].

Glucocorticoids, which are released during chronic stress, can bind to activated NF-κB — inactivating its action, increase the transcription of the IkBα gene, which binds to activated NF-κB, blocking its effect on DNA sites [4].

Aim. To evaluate the activity of NO-synthase isoforms, the concentration of peroxynitrites and nitrosothiols in the soft tissues of the periodontium of rats under the conditions of modeling chronic stress against the background of lipopolysaccharide-induced inflammation.

Methods. Experimental studies were performed on 24 male Wistar rats weighing 190–240 g. The animals were divided into 4 groups: 1 — control, 2 — chronic stress (ChrStr group), animals were kept above water for 1 hour every day for 30 days, 3 — animals that were intraperitoneally injected with 0.4 μg/kg of bacterial LPS of *S. typhi* (pyrogenal) (LPS group) according to scheme described by Mykytenko A.O. et al. [5]; 4 — animals that were simultaneously simulated chronic stress as in group 2 and administered LPS as in group 3 (ChrStr+LPS). The activity of inducible NO-synthase (iNOS), constitutive NO-synthase (cNOS) (Yelinska A.M., 2019), the concentration of nitrosothiols (S-NO) (Gaston B., 1993), and concentration of peroxynitrites of alkali and alkaline earth metals ($ONOO^{\cdot}$) (Akimov O.Y., 2016) were studied in the homogenate of the periodontal soft tissues of rats. The obtained results were subjected to statistical processing using the Mann-Whitney test.

Results. The activity of iNOS in the soft periodontal tissues of rats under chronic stress simulation conditions was increased 1.44 times compared to control group. The activity of iNOS under the conditions of LPS administration was increased 3.88 times compared to the control group. The activity of iNOS under the conditions of combined exposure to chronic stress and LPS was increased 1.95 times compared to the control group (Fig. 1, *A*).

The activity of cNOS in the soft periodontal tissues of rats under chronic stress simulation conditions was decreased by 1.04 times compared to the control group. Activity of cNOS in the periodontal soft tissues of rats under the conditions of LPS administration was increased 3.03 times compared to the control group. Activity of cNOS under conditions of combined exposure to chronic stress and LPS was increased 1.53 times compared to the control group (Fig. 1, *B*).

The concentration of $ONOO^-$ in the soft periodontal tissues of rats under chronic stress simulation conditions was increased 1.46 times compared to the control group (Fig. 2, *A*). The concentration of $ONOO^-$ under the conditions of LPS administration was increased by 1.12 times compared to the control group. The concentration of $ONOO^-$ under conditions of combined exposure to chronic stress and LPS was increased by 1.39 times compared to the control group.

The concentration of nitrosothiols in the soft periodontal tissues of rats under the conditions of chronic stress simulation was decreased by 6.03 times compared to the control group (Fig. 2, *B*). The concentration of nitrosothiols in the periodontal soft tissues of rats under the conditions of LPS administration was decreased by 2.73 times compared to the control group. The concentration of nitrosothiols under conditions of combined exposure to chronic stress and LPS was decreased by 3.15 times compared to the control group.

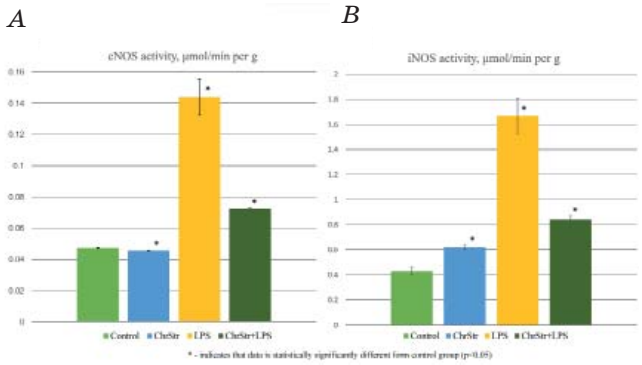

Fig. 1. **The activity of cNOS (*A*) and iNOS (*B*) in the periodontal soft tissues of rats under the conditions of chronic stress simulation against the background of lipopolysaccharide-induced inflammation:**
* — indicates that data is significantly different compared to control group ($P < 0.05$)

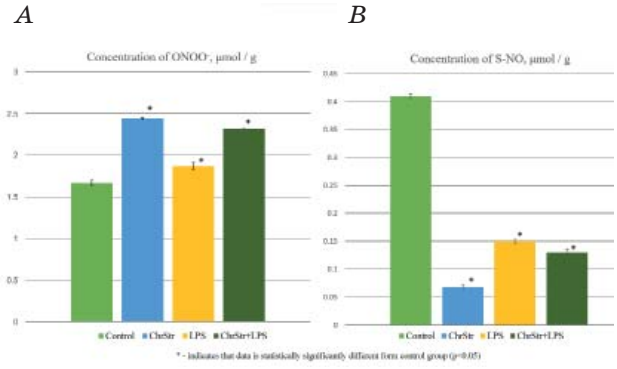

Fig. 2. **The concentration of peroxynitrite (*A*) and nitrosothiols (*B*) in the periodontal soft tissues of rats under the conditions of chronic stress simulation against the background of lipopolysaccharide-induced inflammation:**
* - indicates that data is significantly different compared to control group ($P < 0.05$)

Discussion. The combined effect of chronic stress and bacterial LPS increases iNOS activity relative to the control group due to the interaction of LPS with TLR 4 and the induction of iNOS expression [6]. The combination of chronic stress and bacterial LPS introduction leads to limitation of LPS-induced increase in cNOS and iNOS activities. Simultaneous decrease in cNOS and iNOS activities, observed in this group can lead to lowered concurrence of these enzymes for the substrate of reaction, which in turn decreases chances for cNOS uncoupling. However, the state of cNOS coupling with substrate in our study was not investigated and requires further research. Increase in $ONOO^-$ concentration creates a threat of nitrosative stress development, while decrease in S-NO concentration may lead to microcirculatory disfunction in soft periodontal tissues.

Conclusions. The combined effect of bacterial lipopolysaccharide and chronic stress leads to increased production of nitrogen monoxide from inducible NO-synthase and elevates concentration of reactive forms of nitrogen, which creates possibility for development of nitrosative stress in the soft periodontal tissues.

Keywords: chronic stress; lipopolysaccharide; nitrogen monoxide; periodontal soft tissues.

Authors' contribution. Pletnov V.V. — data gathering, data analysis, data interpretation, writing original draft. Tkachenko O.T. — data gathering, data analysis, data interpretation, writing original draft. Mykytenko A.O. — design and concept, data analysis, statistics, revision and approval of original draft.

REFERENCES

1. *Kim S., Lee J. Y., Park J. Y., Kim Y., Kang C. H.* Lacticaseibacillus rhamnosus MG4706 Suppresses Periodontitis in Osteoclasts, Inflammation-Inducing Cells, and Ligature-Induced Rats. *Nutrients*. 2022, 14(22), 4869. https://doi.org/10.3390/nu14224869
2. *Tarasenko L.M., Petrushanko T.A. Stress and periodontium. Poltava*; 1999. 192 P.
3. *Spector A. M., Postolache T. T., Akram F., Scott A. J., Wadhawan A., Reynolds M. A.* Psychological Stress: A Predisposing and Exacerbating Factor in Periodontitis. *Curr Oral Health Rep*. 2020, v. 7, p. 208–215. https://doi.org/10.1007/s40496-020-00282-2
4. *Barnes P. J., Karin M.* Nuclear factor-kappaB: a pivotal transcription factor in chronic inflammatory diseases. *N. Engl. J. Med.* 1997, 336(15),1066-1071. https://doi.org/10.1056/NEJM199704103361506
5. *Mykytenko A. O., Akimov O. Y., Neporada K. S.* Influence of lipopolysaccharide on the development of oxidative-nitrosative stress in the liver of rats under conditions of chronic alcohol intoxication. *Fiziol Zh*. 2022, 68(2), 29–35. : https://doi.org/10.15407/fz68.02.029
6. *Jin S. J., Song Y., Park H. S., Park K. W., Lee S., Kang H.* Harmine Inhibits Multiple TLR-Induced Inflammatory Expression through Modulation of NF-κB p65, JNK, and STAT1. *Life* (Basel). 2022, 12(12), 2022. https://doi.org/10.3390/life12122022

UDC 577.218+616-006 https://doi.org/10.15407/biotech16.02.042

INCREASED EXPRESSION LEVEL OF ADAPTOR PROTEIN RUK/CIN85 IN DOXORUBICIN-RESISTANT HUMAN NON-SMALL LUNG ADENOCARCINOMA MOR CELLS IS ASSOCIATED WITH THEIR METABOLIC REPROGRAMMING

Y. S. RAYNICH[2], *T. D. SKATERNA*[1], *D. S. GERASHENKO*[1], *O. O. HUDKOVA*[1], *T. O. KISHKO*[1], *N. V. LATYSHKO*[1]

[1]Palladin Institute of Biochemistry of the National Academy of Sciences of Ukraine, Kyiv
[2]Taras Shevchenko National University, Ukraine, Kyiv

E-mail: yanaraynich@gmail.com

Received 2023/03/20
Revised 2023/04/14
Accepted 2023/04/28

One of the most lethal types of cancer in the world is non-small-cell lung carcinoma (NSCLC). This is due to diagnosing of lung cancer mainly at advanced stages associated with increased resistance of cancer cells to traditional anticancer chemotherapeutic drugs as well as their high metastatic potential [1]. We previously showed that overexpression of the adaptor protein Ruk/CIN85 in breast cancer cells is associated with their malignancy and increased chemoresistance [2, 3]. To promote survival under the treatment with anti-cancer drugs, cancer cells dynamically change their metabolism.

Aim. The purpose of the present study was to find out the role of Ruk/CIN85 in modulation of activities/content of key enzymes/components of glycolysis and hydrogen peroxide using as a model human NSCLC MOR wild type and resistant to drugs MOR/0.2R cells.

Materials and Methods. MOR (ECACC 84112312) and MOR/0.2R (ECACC 96042335), drug-resistant cell line, were cultured in the complete RPMI medium under standard conditions. Enzymes activity, content of metabolites and protein in cell extracts and the conditioned cell culture medium were estimated by spectrophotometric and fluorometric assays.

Results and Discussion. First of all, by using RT^2-PCR it was revealed that the level of Ruk/CIN85 mRNA in drug-resistant MOR cells was 10 times higher than in parental MOR cells. As can be seen from Fig. *A, B*, the high expression level of Ruk/CIN85 in MOR/0.2R cells was related to the increased activity/content of markers of aerobic glycolysis (known as the Warburg effect), lactate dehydrogenase A (LDHA) and lactate as well as marker of chemoresistance of cancer stem cells, aldehyde dehydrogenase (ALDH), as compared to control. The activities of lysyl oxidase (LOX) and diamine oxidase (DAO) were also significantly higher in resistant cells (Fig. *C*). It has been shown that these enzymes are associated with aggressiveness of tumor cells. In particular, the activity of LOX is related to the increased degree of stiffness of the extracellular matrix, while the activity of DAO is involved in the control of cell proliferation [4, 5]. Significant increase in the level of hydrogen peroxide in the MOR/0.2R cells (Fig. *D*) may be, at least partially, associated with increased activities of amine oxidases studied as one of the products of the enzymatic reaction. Based on the obtained results, we draw a conclusion that observed changes in the intensity of glycolysis, amine oxidases activities and content of hydrogen peroxide in doxorubicin-resistant MOR/0.2R cells positively correlate with the expression level of the adaptor protein studied.

Conclusions. In conclusion, it can be assumed that the adaptor protein Ruk/CIN85 is involved in metabolome reprogramming and may function as an important component of regulatory networks required for the acquisition of drug resistant phenotype by NSCLC cells.

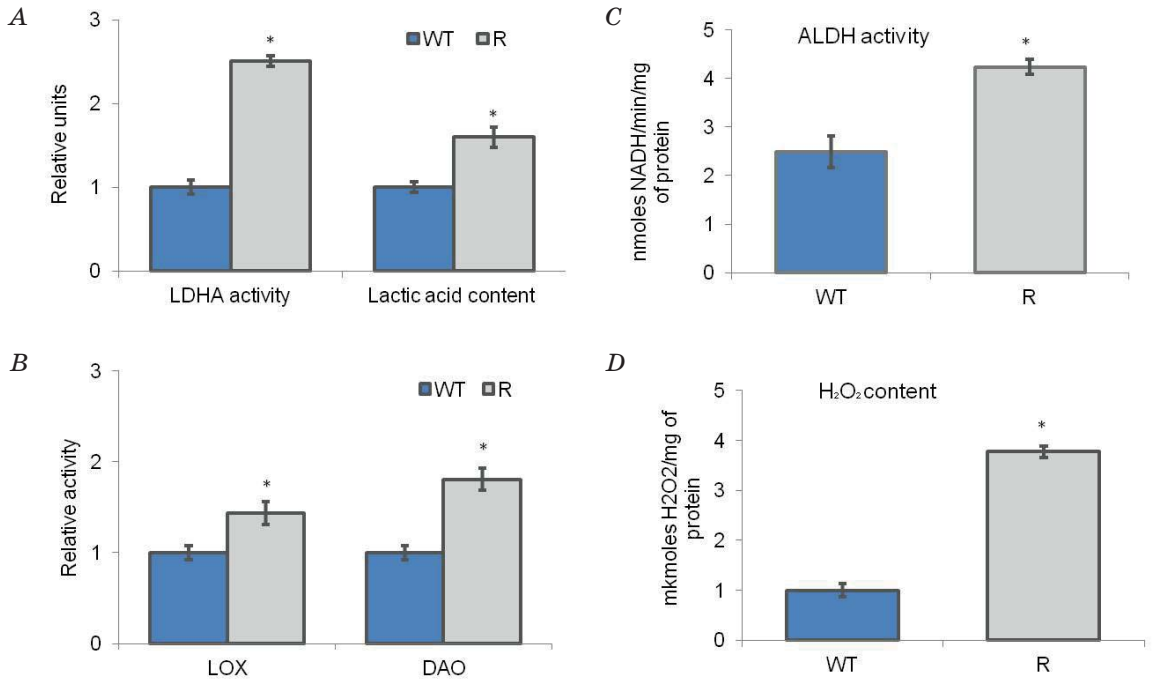

Figure. **Increased level of adaptor protein Ruk/CIN85 in MOR/0.2R cells positively correlates with metabolic parameters that potentially ensure their chemoresistance:**
$M \pm m$, $n = 3$, * — $P < 0.05$ compared to the corresponding control

Key words: non-small-cell lung carcinoma (NSCLC); adaptor protein Ruk/CIN85; chemoresistance; metabolome reprogramming; metabolic enzymes; hydrogen peroxide.

Acknowledgments. We express our gratitude to Professor Liudmyla Drobot for scientific guidance and support of our work.

Funding. The research was financed by the project No. 0120U002191 supported by the National Academy of Sciences of Ukraine.

REFERENCES

1. *Hanahan D., Weinberg R. A.,* Hallmarks of cancer: the next generation. *Cell*, 2011, 144(5), 646–674. https://doi.org/10.1016/j.cell.2011.02.013
2. *Samoylenko A., Vynnytska-Myronovska B., Byts N., Kozlova N., Basaraba O., Pasichnyk G., Palyvoda K., Bobak Y., Barska M., Mayevska O., et al.* Increased levels of the HER1 adaptor protein Rukl/CIN85 contribute to breast cancer malignancy. *Carcinogenesis*, 2012, v. 33, p. 1976–1984. https://doi.org/10.1093/carcin/bgs228
3. *Horak I. R., Gerashchenko, D. S., Drobot L. B.* Adaptor protein Ruk/CIN85 modulates resistance to doxorubicin of murine 4T1 breast cancer cells. *The Ukr. Biochem. J.*, 2018; 90(3), p. 94–100. https://doi.org/10.15407/ubj90.03.094
4. *Liburkin-Dan T., Toledano S., Neufeld G.* Lysyl Oxidase Family Enzymes and Their Role in Tumor Progression. *Int. J. Mol. Sci.* 2022, 23(6249). 1–14. https://doi.org/10.3390/ijms23116249
5. *Xu F., Xu Y., Xiong J-H., Zhang J-H., Wu J., Luo J., Xiong J-P.* AOC1 Contributes to Tumor Progression by Promoting the AKT and EMT Pathways in Gastric Cancer. *Cancer Management and Research*. 2020, v. 12, p. 1789–1798. https://doi.org/10.2147/CMAR.S225229

UDC 57.022, 57.023 https://doi.org/10.15407/biotech16.02.044

STARVATION DURING DEVELOPMENT AFFECTS METABOLISM IN DROSOPHILA

N. P. STEFANYSHYN, O. M. STRILBYTSKA, U. V. SEMANIUK, N. I. BURDYLIUK, S. V. KHARUK

Vasyl Stefanyk Precarpathian National University, Ivano-Frankivsk, Ukraine

E-mail: nadya_stefanyshyn@ukr.net

Received 2023/03/29
Revised 2023/04/21
Accepted 2023/04/28

Nutrition during early stages of development has a strong long-term impact on the adult organism in *Drosophila* and rodents [1–3]. Numerous studies showed, that the effects caused by parental diet could be transmited through generations and modulate lifespan and metabolism in their offspring [1, 4]. Epigenetic control is the most plausible mechanism to explain the effects of parental or developmental nutrition on offspring life-history traits [2, 5].

Aim. In the present work, we aimed to investigate how starvation during early stage of fly development affects carbohydrate metabolism in imago flies and their progeny of F1 generation.

Methods. Wild-type *Canton-S* strain *Drosophila melanogaster* flies were used in all experiments. Flies aged 5–6 days were subjected to two-hours eggs-laying on the standard medium composed of sucrose — 5%, yeast — 5%, agar-agar — 1%, nipagin — 0.18% and reared at 25 °C, relative humidity of 60–70% on a 12 h day/night cycle [6]. After 72 hours of development, we selected third instar larvae and placed them on Petri dishes filled with agar-agar (1%). Experimental larvae were subjected to six-hours starvation, control larvae were not subjected to starvation. Next, larvae were transferred into plastic tubes with standard medium. The four-day-old flies of the parental generation were divided into two subgroup cohorts. One cohort was frozen in liquid nitrogen for biochemical assays. The rest of the parental flies were combined for mating and egg laying. Offspring F1 larvae were allowed to develop on regular food. The 5-day-old offspring were frozen in liquid nitrogen for biochemical measurements. Flies of parental and offspring generations were used for the determination of glycogen and glucose content using the diagnostic kit Glucose-Mono-400-P according to the manufacturer's instructions.

Results represent as the mean ± SEM of 3–4 replicates per group. Asterisk indicates a significant difference between groups with $p < 0.05$ according Student's t-test. Graphing and statistical analysis were performed by using GraphPad Prism.

Results. Starvation during development significantly influenced the level of hemolymph and body glucose in imago flies of parental generation. Hemolymph glucose concentration was lower by 34% ($p = 0.008$) and 32% ($p = 0.033$) in experimental females and males, respectively, as compared to control groups (Fig. *A*). Starvation during development led to lower level of body glucose in adult parental flies of both sexes (Fig. *B*; $p = 0.015$; $P = 0.004$). Adult males F1, generated by parents that were starved during development, showed 3-fold lower glycogen content, as compared to control (Fig. *F*; $P = 0.001$).

Discussion. Here we showed that, starvation during early development modulate the metabolic profile of adult flies. Previous study showed that high-carbohydrate developmental diet led to increase in hemolymph glucose concentration in imago flies [3]. Moreover, larval starvation can determine the feeding behavior of both larvae and adult *Drosophila* [7]. Another study showed decreased level of glycogen, trehalose and free glucose under starvation of third instar larvae [8]. Our data is in a good agreement with previous studies and detect low amount of body glucose in imago males and females caused by larval starvation. Glycogen of the fly fat body is used to maintain homeostasis of glucose under starvation [8]. We found low glycogen pool in adult F1 males. This effect is caused by starvation of the parents during larval stage. Changes in offspring metabolism caused by parental nutrition may be associated with an altered chromatin state [9].

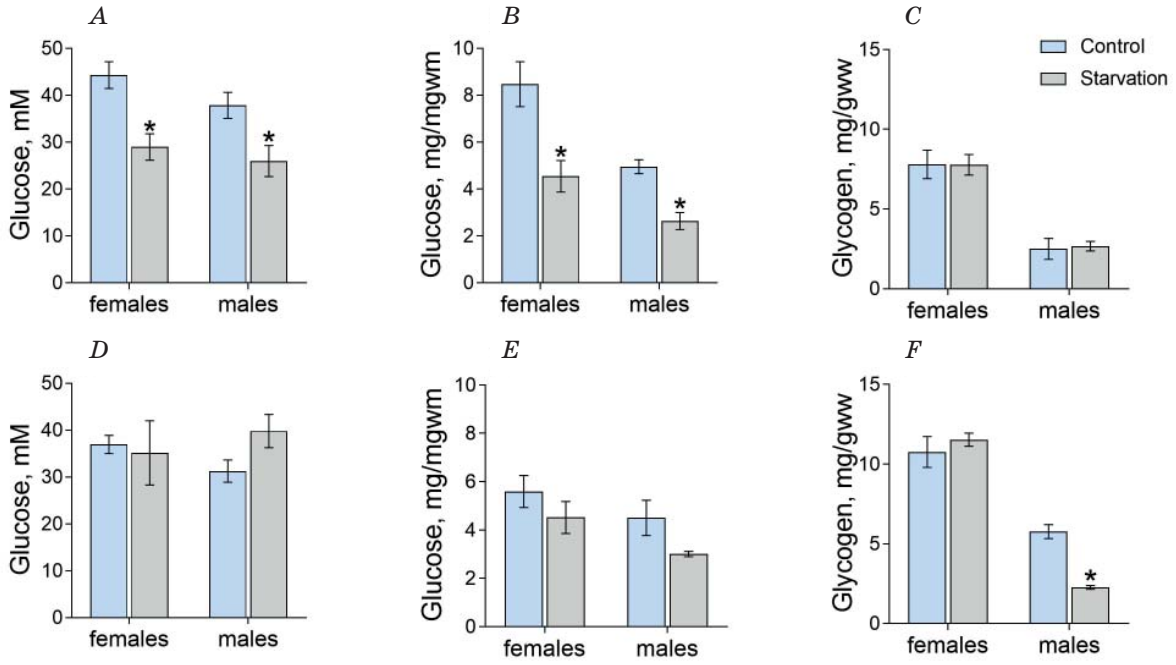

Figure. **The levels of hemolymph glucose (*A*), body glucose (*B*), glycogen (*C*) in imago flies of parental generation Drosophila which were starved for 6 hour in the third larval instar and levels of hemolymph glucose (*D*), body glucose (*E*), glycogen (*F*) in progeny of F1 generation:**
Results are represented as the mean ± SEM of 3–4 replicates per group

Conclusions. Starvation at early stage of development led to lower hemolymph glucose and body glucose level in imago flies. Moreover, parental starvation decreased glycogen pool in F1 males.

Key words: *Drosophila*; development; diet; starvation; nutrition.

Authors' contribution. O. M. Strilbytska, U. V. Semaniuk, N. I. Burdyliuk were responsible for the experimental part of the work, N. P. Stefanyshyn participated in the experimental part of the work and writing theses, S. V. Kharuk carried out graphic and statistical data processing.

Funding. This study was carried out at the department of Biochemistry and Biotechnology, Vasyl Stefanyk Precarpathian National University and the research had no sponsor support.

REFERENCES

1. *Martin-Gronert M. S., Tarry-Adkins J. L., Cripps R. L., Chen J. H., Ozanne S. E.* Maternal protein restriction leads to early life alterations in the expression of key molecules involved in the aging process in rat offspring. *Am. J. Physiol. Regul. Integr. Comp. Physiol.* 2008, 294 (2), R494–500. https://doi.org/10.1152/ajpregu.00530.2007
2. *Vaiserman A., Lushchak O.* Prenatal Malnutrition-Induced Epigenetic Dysregulation as a Risk Factor for Type 2 Diabetes. *Int. J. Genomics.* 2019, 3821409. https://doi.org/10.1155/2019/3821409
3. *Strilbytska O. M., Semaniuk U. V., Burdyliyk N. I., Bubalo V., Lushchak O. V.* Developmental diet defines metabolic traits in larvae and adult *Drosophila*. *The Ukr. Biochem. J.* 2022, 94 (1), 53–63. https://doi.org/10.15407/ubj94.01.053
4. *Strilbytska O., Velianyk V., Burdyliuk N., Yurkevych I. S., Vaiserman A., Storey K. B. Pospisilik A., Lushchak O.* Parental dietary protein-to-carbohydrate ratio affects offspring lifespan and metabolism in drosophila. *Comp. Biochem. Physiol. A Mol. Integr. Physiol.* 2020, 241, 110622. https://doi.org/10.1016/j.cbpa.2019.110622
5. *Vaiserman A., Lushchak O.* Developmental origins of type 2 diabetes: Focus on epigenetics. *Ageing Res Rev.* 2019, 55, 100957. https://doi.org/10.1016/j.arr.2019.100957

6. *Rovenko B. M., Perkhulyn N. V., Lushchak O. V., Storey J. M., Storey K. B., Lushchak V. I.* Molybdate partly mimics insulin-promoted metabolic effects in *Drosophila melanogaster*. *Comp. Biochem. Physiol. C Toxicol. Pharmacol.* 2014, 165, 76–82. https://doi.org/10.1016/j.cbpc.2014.06.002
7. *Ahmad M., Chaudhary S.U., Afzal A.J., Tariq M.* Starvation-Induced Dietary Behaviour in *Drosophila melanogaster* Larvae and Adults. *Sci. Rep.* 2015, 5, 14285. https://doi.org/10.1038/srep14285
8. *Yamada T., Habara O., Kubo H., Nishimura T.* Fat body glycogen serves as a metabolic safeguard for the maintenance of sugar levels in *Drosophila*. *Development*. 2018, 145 (6), dev158865. https://doi.org/10.1242/dev.158865
9. *Ost A., Lempradl A., Casas E., Weigert M., Tiko T., Deniz M., Pantano L., Boenisch U., Itskov P. M., Stoeckius M., Ruf M., Rajewsky N., Reuter G., Iovino N., Ribeiro C., Alenius M., Heyne S., Vavouri T., Pospisilik J. A.* Paternal diet defines offspring chromatin state and intergenerational obesity. *Cell*. 2014, 159 (6), 1352–1364. https://doi.org/10.1016/j.cell.2014.11.005

UDC 618.2: 577.29 **https://doi.org/10.15407/biotech16.02.047**

FIBRINOLYTIC POTENTIAL INCREASING DURING ACTIVATION OF BLOOD COAGULATION IN THE COURSE OF PREGNANCY WITH PLACENTAL DYSFUNCTION

Y. TSARYK[1, 2], *I. US*[3]

[1]Palladin Institute of biochemistry of the National Academy of Sciences of Ukraine, Kyiv
[2]Educational and Scientific Center "Institute of Biology and Medicine", Kyiv, Ukraine
[3]Shupyk National Medical Academy of Postgraduate Education, Kyiv, Ukraine

E-mail: alfiemeier@gmail.com

Received 2023/03/17
Revised 2023/04/26
Accepted 2023/04/28

Hemostasis is an integrative system that supports the blood flow in the vessels and the effective termination of bleeding during trauma. Primary hemostasis, secondary hemostasis and the fibrinolytic system are the three main components of blood coagulation. Pathological activation of blood coagulation can lead to the intravascular thrombus formation. On the other hand, the suppression of blood coagulation can lead to the bleeding disorders. Both thrombosis and hemorrhages are dangerous conditions that can cause severe illness or even death. The dynamic balance in hemostatic system is extremely important during such physiological condition as pregnancy. Any disruption of this balance can be dangerous for mother and for fetus. However, in obstetric clinical practice today especially hypo- and hyper-fibrinolytic disorders are probably underdiagnosed because of lack of knowledge and lack of accurate diagnostic tests [4]. So, the study of molecular mechanisms of hemostasis balance is one of the most vivid tasks for clinical biochemistry.

Aim. In present work we aimed to underline the constant connection between blood coagulation and fibrinolysis.

Methods. Blood samples of women with placental disfunction during pregnancy ($n = 28$) were kindly provided by "Perinatal Center of Kyiv". This study was approved by the Ethics Commission of the Shupyk National Medical Academy of Postgraduate Education and the Ethics Commission of the Kyiv Perinatal Center (# 3 from 05/05/2020).

Blood coagulation activation was estimated by the accumulation of Soluble Fibrin (SF). Highly sensitive and effective immunochemical method for the determination of soluble fibrin by sandwich ELISA was used. As the catch-antibody we used fibrin-specific mAb FnI-3C. As the tag-antibody we used another mAb (II-4d) that has an epitope in the NH 2 -terminal fragment of the γ-chain of the D-region of the fibrin(ogen) molecule. This approach allowed performing quantitative determination in human blood plasma of soluble fibrin that is composed of monomers, dimers and oligomers of fibrin, possibly with fibrinogen molecules at the sticky ends and also initial products of plasmin hydrolysis of fibrin [1, 2].

The rate of activation of fibrinolysis was estimated by measuring of Fibrinolytic Potential (FP). It was measured by turbidimetric method with recording the scattering of light by a fibrin clot at 405 nm on a microplate reader Multiscan (Finland). The clot was formed in the microplate wells in blood plasma activated by APTT reagent in the presence or without t-PA.

The area under the turbidity curve of the clot from the moment of initiation of plasma coagulation to the moment of complete destruction of the clot in the presence of t-PA indicated the Overall hemostasis potential (OHP). Coagulation potential (CP) was the area under the curve of clot formation from the moment of initiation of plasma coagulation to the moment of complete dissolution of the clot in the absence of t-PA. Fibrinolytic potential (FP) was the difference between the values of CP and OHP. As the area under the curves these parameters are being measured in optical units *per* second (ou/s) [3].

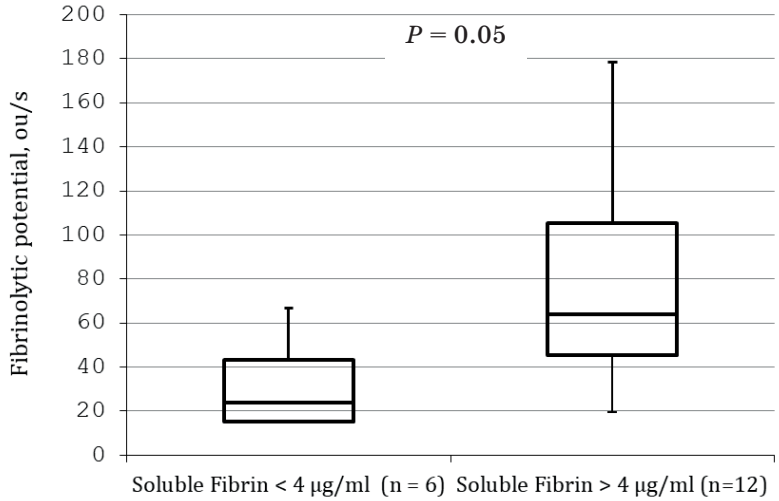

Figure. **Fibrinolytic Potential of blood plasma of pregnant women with placenta dysfunction that had increased vs normal concentration of Soluble Fibrin**

Statistical analysis was performed according to Mann-Whitney U test.

Results. SF was found in blood plasma of 12 pregnant women with placenta dysfunction. Six of studied patients had SF less than 4 μg/ml that were assumed as the control meanings [5]. We divided patients on two groups according to this parameter. It was shown that patients of the 1st group (SF ≤ 4) exhibited FP as 24 ou/s. In the same time patients of the 2nd group (SF ≥ 4) had much higher FP — 62 ou/s. The level of statistical significance was $P = 0.05$.

Discussion. In normal pregnancy, there is a marked increase in the procoagulant activity in maternal blood characterized by elevation of factors VII, X, VIII, fibrinogen and von Willebrand factor, which is maximal around term. This is associated with an increase in prothrombin fragments (PF1+2) and thrombin–antithrombin complexes [6]. Changes in the hemostasis system under the conditions of pregnancy with pathologies remains an actual topic and requires research. Some studies demonstrate that disorders during pregnancy (for example, preeclampsia) are characterized by changes in the t-PA/PAI-1 system indicating an endothelial dysfunction [7]. Our study revealed an interesting interrelation between FP and SF (more SF — higher FP) in the blood system of pregnant women with placental dysfunction. We assume that this is the sign of mutual regulation between coagulation and fibrinolysis in hemostasis. In our opinion, the activation of blood coagulation system (which can be estimated by the accumulation of SF) leads to the activation of fibrinolysis. Such compensatory activation is needed for effective dissolution of any clot that can appear in the bloodstream. It is unclear if the SF as the oligomers of fibrin can stimulate fibrinolysis directly, or some other mechanisms of interconnection are involved. The introduction of a complex indicator into laboratory practice, taking into account CP and FP, will allow more adequately assessing the presence of a thrombophilic state in patients with vascular-placental disorders and preventing the development of such complications.

Conclusions. Blood coagulation activation (estimated by SF measurement) was shown to be accompanied by fibrinolysis activity increasing (measured by FP evaluation) in pregnant women with placental dysfunctions. These findings can be evidence of constant balance between blood coagulation and fibrinolysis that stabilize hemostasis in pathological conditions for avoiding thrombosis or hemorrhages.

Keywords: soluble fibrin; pregnancy; fibrinolysis; fibrinolytic potential; blood coagulation.

Ethical Committee Approval: # 3 from 05/05/2020

Acknowledgement. Authors gratefully acknowledge Prof. S. I. Zhuk and Dr. V. O. Chernyshenko for their contribution to this work.

Author's contribution. Y. Tsaryk performed soluble fibrin and overall hemostatic potential measuring, I. Us supervised and monitored the patients.

Funding. The research was financed by the project No. 0119U002512 "The interaction of the hemostasis system components at the cellular and molecular level in the process of formation and elimination of a thrombus".

REFERENCES

1. *Lugovskoy E. V., Kolesnikova I. N., Komisarenko S. V.* Usage of monoclonal antibodies for determination of localization of antigenic determinants and fibrin polymerization sites within fibrinogen and fibrin molecules and their application in test-systems for diagnostics and the threat of thrombus formation. *Biotechnologia Acta*. 2013, 6(4), 33–42. https://doi.org/10.15407/biotech6.04.033
2. *Lugovskoi E. V, Gritsenko P. G., Komisarenko S. V.* Molecular mechanisms of the polymerization of fibrin and the formation of its three-dimensional network. *Bioorg Khim*. 2009, 35(4), 437–456.
3. *Storozhuk N. V., Pyrogova L. V., Chernyshenko T. M., Kostyuchenko O. P., Platonova T. M., Storozhuk O. B., Storozhuk B. G., Marunich R. Yu., Bereznytsky G. K., Makogonenko E. M.* Overall hemostasis potential of blood plasma and its connection to molecular markers of the hemostasis system in patients with stenosis of coronary artery. *The Ukr. Biochem. J*. 2021, 93(5), 31–42. https://doi.org/10.15407/ubj93.05.031
4. *Saes J. L, Schols SEM, van Heerde W. L, Nijziel M. R.* Hemorrhagic disorders of fibrinolysis: a clinical review. *J. Thromb. Haemost*. 2018, v. 16, p. 1498–1509. https://doi.org/10.1111/jth.14160 Online ahead of print.
5. *Komisarenko S. V., Deev V. A. Lugovskoy E. V., Kolesnikova I. M., Platonova T. M. Lugovska N. E., Kostyuchenko O. P., Chernyshenko V. O., Koroleva D. S., Chernyshenko T. M., Liksunov O. V., Kashirova O. V., Romanov E. E.* Application of immunoenzymatic methods for laboratory diagnosis of the threat of intravascular thrombus formation. 2019, *Kyiv, Publisher Byhun V. Yu.*, p. 16.
6. *Brenner B.* Haemostatic changes in pregnancy. *Special issue — State-of-the-Art 11th International Congress on Antiphospholipid Antibodies*, 2004, 114 (5–6), 409–114.
7. Godtfredsen, Anne Cathrine et al. "Fibrinolytic Changes in Women with Preeclampsia"; Clinical and applied thrombosis/hemostasis : official journal of the International Academy of Clinical and Applied Thrombosis/Hemostasis 2022, 28. 10760296221126172.

UDC 612.115:612.128 https://doi.org/10.15407/biotech16.02.050

DETERMINATION OF THROMBIN AND PLASMIN ACTIVITY IN HUMAN BLOOD PLASMA USING THE TURBIDIMETRIC CURVE OF CLOT FORMATION AND DISSOLUTION

A. V. UDOVENKO

Paladin Institute of Biochemistry of the National Academy of Sciences of Ukraine, Kyiv

E-mail: nudovenko26@gmail.com

Received 2023/03/09
Revised 2023/04/03
Accepted 2023/04/28

Thrombin and plasmin are the terminal enzymes of the activation pathway of the coagulation and fibrinolysis systems of human blood plasma, respectively. Their concentrations indicate the degree of functional readiness of each of the systems to respond to disturbances in the hemostasis system, and the ratio of the rates of formation and dissolution of a plasma clot *in vitro* indicates the degree of balance between the coagulation and fibrinolysis systems (1). Thrombin is a multifunctional enzyme, which prompted the development of numerical methods for determination its concentration in blood plasma, using predominantly the enzyme amidase activity to peptide substrates labeled by p-nitroaniline (pNA) or fluorescent mark (*1, 2*). However, it was shown that the curve of amidase activity for thrombin does not coincides with such of clot turbidity. Therefore, the method of determining the rate of activation and concentration of thrombin based on its amidase activity does not reflect the rate of activation of thrombin in the initial period of blood plasma coagulation, in which protofibrils are formed and thrombin activity is directed only to the formation of fibrin. The thrombin, formed by the coagulation system in the lag period, exhibits maximum activity in relation to the fibrinogen substrate, while the rate of protofibril formation depends on the thrombin concentration.

Aim. The purpose of the work was to develop a method for determination the activity of thrombin, which is based on the turbidimetry curve (TDC) of the formation and dissolution of a blood plasma clot. At the same time, the theoretical analysis of the dissolution phase of the blood plasma clot by the fibrinolytic system allowed to propose a method for determination the concentration of the formed plasmin using its amidase activity.

Methods. Donor blood samples were collected in 3.8% sodium citrate (1 part of sodium citrate and 9 parts of blood, pH 7.4). Plasma was separated from blood cells within 1 hour after blood collection by centrifugation the latter at 1200 g for 20 min. Aliquots of plasma were stored at −20 °C.

Blood plasma coagulation was studied by the turbidimetric method by recording the turbidity of the fibrin clot at 405 nm on a SF 2000 spectrophotometer.

The clots were formed in plastic cuvettes, into which 0.05 M HEPES buffer containing 0.15 M NaCl, 0.005% Tween-20, pH 7.4, 40 µl of blood plasma, t-PA to a final concentration of 75 IU/ml and 50 µl of APTT reagent were added. The plasma coagulation process was initiated by adding 25 mM $CaCl_2$. The final volume of the reaction mixture was 400 µl. Processing of the results was performed a standard statistical program in *Excel*. The mean values of the parameters and their standard deviation were determined.

Results. To determine the concentrations of thrombin and plasmin, TDCs of the formation and dissolution of blood plasma clots, initiated by the APTT reagent, were used. A typical experiment in which TDC was used to determine τ values at thrombin concentrations from 0.1 to 0.5 NIH per mlb is shown in the Fig. Based on τ values obtained in 3 experiments, a calibration curve was constructed in the coordinates $1/\tau$ — [Thr] (the rate of protofibrils formation in s^{-1} vs thrombin concentration in NIH units in 1 ml). The activity of thrombin — 1 NIH in 1 ml — corresponded to a concentration of 27,7 nM.

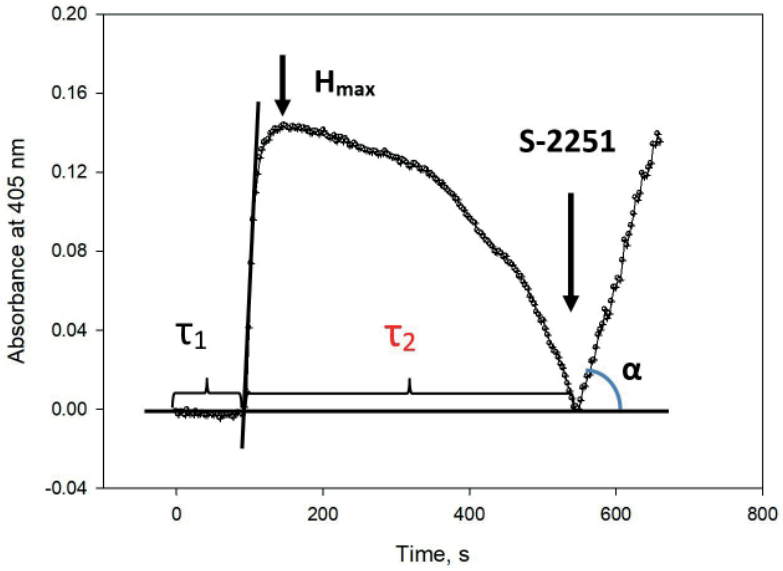

Figure. **Determination of thrombin and plasmin activity, which are formed during the formation and dissolution of a fibrin clot in blood plasma in the presence of t-PA and the peptide substrate S 2251 (H-D-Val--Lys-pNA), added at the moment of complete dissolution of the clot, using parameter τ and amidase activity of plasmin (V), respectively:**

τ_1 — lag period of clot formation; τ_2 — time of clot existence; H_{max} — maximum clot turbidity, point of transition from clot formation stage to clot dissolution stage; S-2251 — moment of introduction of plasmin substrate into the dissolved clot; α — angle of inclination of S-2251 cleavage curve to the abscissa axis; tgα is equal to the amidase activity of the formed plasmin (V)

In 6 independent experiments based on TDC, the following values of τ and V for thrombin and plasmin were found, respectively, 0.095±8.83 s^{-1} and 0.062±0.12 optical units (o.u.)/min, which corresponded to their concentrations of 2.77 nM for thrombin and 22.3 nM for plasmin. Considering that the concentration of prothrombin and Glu-Pg in the reaction medium was 100 and 140 nM, respectively, the% concentrations of activated thrombin and plasmin to such of proenzymes were 2.9% and 15.9%, respectively. The thrombin concentration ratio to such of plasmin was ~ 1:8. It turned out to be sufficient activation 2.9% concentration of prothrombin for the protofibrils formation, and 15.9% concentration of Glu-Pg for complete dissolution of the clot.

Discussion. Activity and concentration of thrombin were determined by its ability to transform the natural substrate fibrinogen into fibrin and form the basic structure of the clot — protofibrils. Determination of plasmin activity was based on direct measurement of plasmin amidase activity at the moment when the three-dimensional structure of the plasma clot was completely destroyed and the optical density in the cuvette reached zero. Calculation of plasmin activity was carried out based on data of the plasmin standard specific amidase activity. Amidase activity (substrate S-2251) of the plasmin standard was 0.033 o.u. of pNA released by 1 μg/ml of enzyme per 1 minute at 405 nm. Then the concentration of plasmin was

$$C = \frac{\Delta E_{405}\ o.u.}{N_{min}*0.033\ o.u./(\frac{\mu g}{ml}*\text{min})} = \frac{\Delta E_{405}}{N*0.033}$$ μg/ml, where

N_{min} — duration of measurement of plasmin activity in minutes;
ΔE405 o.u. — growth of the optical density in the cuvette during the measurement;
0.033 o.u./(μg/ml*min) — rate of p-NA release by 1 μg/ml of plasmin per 1 min.

Conclusion. The proposed methods to determine the activity of thrombin and plasmin made it possible to quantitatively calculate the rate of prothrombin activation in the lag period, the concentration and activity of thrombin based on the rate of fibrin and protofibrils formation as well as the activity and concentration of plasmin at the point of the complete clot dissolution,

the average rate of activation of plasminogen during the destruction of the clot structure and the time of formation and dissolution of the three-dimensional structure of the clot.

Key words: thrombin; plasmin; blood plasma coagulation; hemostasis; coagulation; fibrinolysis.

Acknowledgement. I am grateful to Prof. E.M. Makogonenko for supervising my research.

Author's contribution. A.V. Udovenko performed experiments, calculations and analysis of results and writing theses.

Founding. The research was financed by the project 0119U002512 of Palladin Institute of Biochemistry of the National Academy of Sciences of Ukraine.

REFERENCES

1. *van Geffen M., Loof A., Lap P., Boezeman J., Laros-van Gorkom B. A., Brons P., Verbruggen B., van Kraaij M., van Heerde W. L.* A novel hemostasis assay for the simultaneous measurement of coagulation and fibrinolysis. *Hematology* 2011, v. 16, 327–336. https://dpi.org/10.1179/102453311X13085644680348
2. *Matsumoto T., Nogami K., Shima M.* Simultaneous measurement of thrombin and plasmin generation to assess the interplay between coagulation and fibrinolysis. *Thromb Haemost* 2013, v. 110, 761–768. https://dpi.org/10.1160/Tj2H13-04-0345